

NTL
49868

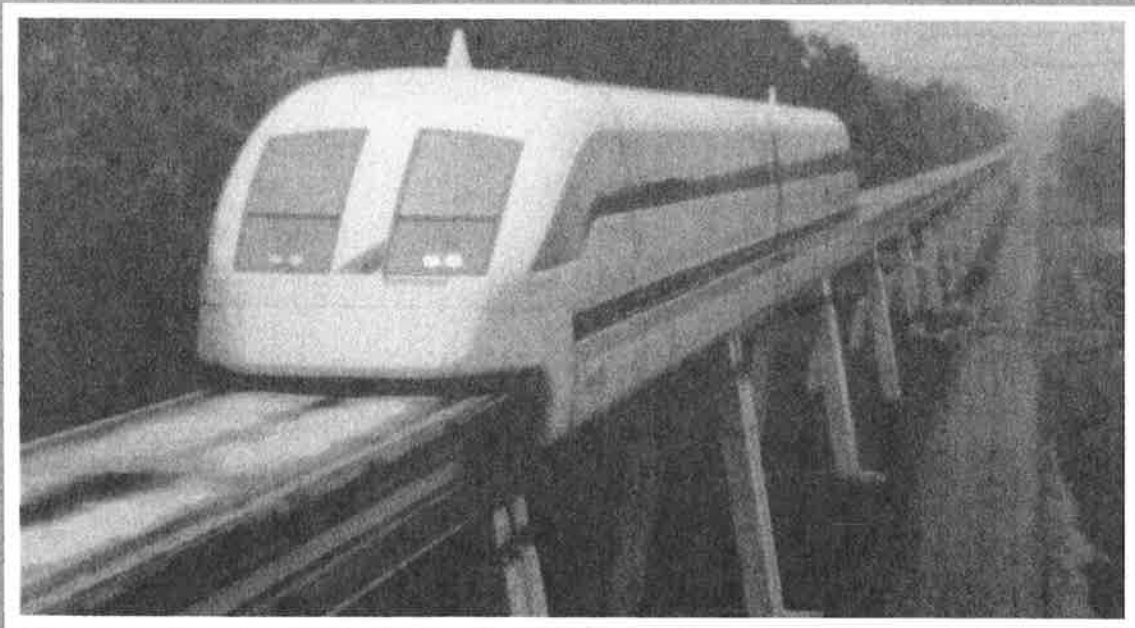


U. S. Department
of Transportation
Federal Railroad
Administration

Safety of High Speed Magnetic Levitation Transportation Systems

Office of Research
and Development
Washington D.C. 20590

Thermal Effects and Related Safety Issues of Typical Maglev Steel Guideways



DOT/FRA/ORD-94/10
DOT-VNTSC-FRA-94-9

Final Report
September 1994

This document is available to the
public through the National Technical
Information Service, Springfield, VA 22161

④ Safety
Thermal

NOTICE

This document is disseminated under the sponsorship of the Department of Transportation in the interest of information exchange. The United States Government assumes no liability for its contents or use thereof.

NOTICE

The United States Government does not endorse products or manufacturers. Trade or manufacturers' names appear herein solely because they are considered essential to the object of this report.

NOTICE

This document is advisory in nature. The recommended guidelines contained herein do not have the force and effect of law or regulation.

REPORT DOCUMENTATION PAGE

Form Approved
OMB No. 0704-0188

Public reporting burden for this collection of information is estimated to average 1 hour per response, including the time for reviewing instructions, searching existing data sources, gathering and maintaining the data needed, and completing and reviewing the collection of information. Send comments regarding this burden estimate or any other aspect of this collection of information, including suggestions for reducing this burden, to Washington Headquarters Services, Directorate for Information Operations and Reports, 1215 Jefferson Davis Highway, Suite 1204, Arlington, VA 22202-4302, and to the Office of Management and Budget, Paperwork Reduction Project (0704-0188), Washington, DC 20503.

1. AGENCY USE ONLY (Leave blank)		2. REPORT DATE September 1994		3. REPORT TYPE AND DATES COVERED Final Report January 1993-November 1993	
4. TITLE AND SUBTITLE Safety of High Speed Magnetic Levitation Transportation Systems: Thermal Effects and Related Safety Issues of Typical Maglev Steel Guideways				5. FUNDING NUMBERS R4020/RR493	
6. AUTHOR(S) S.J. Kokkins, A. Purple, G. Samavedam					
7. PERFORMING ORGANIZATION NAME(S) AND ADDRESS(ES) Foster-Miller, Inc. * 350 Second Avenue Waltham, MA 02154-1196				8. PERFORMING ORGANIZATION REPORT NUMBER DOT-VNTSC-FRA-94-9	
9. SPONSORING/MONITORING AGENCY NAME(S) AND ADDRESS(ES) U.S. Department of Transportation Federal Railroad Administration Office of Research and Development Washington, DC 20593				10. SPONSORING/MONITORING AGENCY REPORT NUMBER DOT/FRA/ORD-94/10	
11. SUPPLEMENTARY NOTES *under contract to: U.S. Department of Transportation Research and Special Programs Administration John A. Volpe National Transportation Systems Center Cambridge, MA 02142-1093					
12a. DISTRIBUTION/AVAILABILITY STATEMENT This document is available to the public through the National Technical Information Service, Springfield, VA 22161				12b. DISTRIBUTION CODE	
13. ABSTRACT (Maximum 200 words) <p>This report presents a theoretical analysis predicting the temperature distributions, thermal deflections and thermal stresses that may occur in typical steel Maglev guideways under the proposed Orlando, FL thermal environment. Transient, finite element heat transfer analyses are used to predict the thermal response of a typical steel guideway design similar to the Transrapid design being finalized for the Orlando, FL Maglev system. Parametric studies are conducted to examine the sensitivity of the temperature distributions and thermal deflections to time varying changes in the sun's position, seasonal changes, and changes in the guideway orientation and surface treatment. Related safety issues are also addressed.</p> <p>The results of these analyses indicate that the depthwise temperature gradient is steep and nonlinear, which can result in thermal deflections up to 13 mm for single spans. Parametric study results indicate that the vertical deflections are greatest at the spring/fall equinox for East-West orientations, but are also in the 10 to 11 mm range in summer when the guideway is oriented in the North-South direction. The horizontal deflections up to 8 mm are greatest in winter when the guideway is oriented in the East-West direction. The use of double spans is shown to reduce the guideway deflections, but also increase the bending stresses. Application of a white coating to the guideway is shown to reduce the guideway temperatures, deflections and stresses and is strongly dependent on thermal properties of the coatings. The effects of vehicle heating may be expected to worsen guideway deflections but detailed study is required in further work. The effects of ground radiation slightly reduce the guideway deflections, and are shown to affect the guideway primarily when it is mounted close to ground level on short pylons.</p>					
14. SUBJECT TERMS Thermal, guideway, Maglev, temperature, deflection, Transrapid				15. NUMBER OF PAGES 89	
				16. PRICE CODE	
17. SECURITY CLASSIFICATION OF REPORT Unclassified	18. SECURITY CLASSIFICATION OF THIS PAGE Unclassified	19. SECURITY CLASSIFICATION OF ABSTRACT Unclassified	20. LIMITATION OF ABSTRACT		

PREFACE

The report presents a comprehensive theoretical study of the thermal response of the Transrapid steel guideway proposed for use in Orlando, FL. The work was performed under the OMNI Contract DTRS-57-89-D000089 awarded by Volpe National Transportation Systems Center, (VNTSC) in Cambridge, MA. The work was sponsored by the Office of Research and Development, Federal Railroad Administration, U.S. Department of Transportation at Washington, D.C. under the overall direction of Mr. Arne Bang, Program Manager. The COTR for this program was Dr. Andrew Kish of VNTSC. Supporting this program at Foster-Miller was Dr. David Cope, who assisted in the analysis of guideway heating by stator packs. Thanks are also due to Dr. David Wormley, who is Foster-Miller's consultant on this project.

SI* (MODERN METRIC) CONVERSION FACTORS

APPROXIMATE CONVERSIONS TO SI UNITS

APPROXIMATE CONVERSIONS FROM SI UNITS

Symbol	When You Know	Multiply By	To Find	Symbol	When You Know	Multiply By	To Find	Symbol
LENGTH								
in	inches	25.4	millimeters	mm	millimeters	0.039	inches	in
ft	feet	0.305	meters	m	meters	3.28	feet	ft
yd	yards	0.914	meters	m	meters	1.09	yards	yd
mi	miles	1.61	kilometers	km	kilometers	0.621	miles	mi
AREA								
in ²	square inches	645.2	millimeters squared	mm ²	millimeters squared	0.0016	square inches	in ²
ft ²	square feet	0.093	meters squared	m ²	meters squared	10.764	square feet	ft ²
yd ²	square yards	0.836	meters squared	m ²	meters squared	1.195	square yards	ac
ac	acres	0.405	hectares	ha	hectares	2.47	acres	mi ²
mi ²	square miles	2.59	kilometers squared	km ²	kilometers squared	0.386	square miles	
VOLUME								
fl oz	fluid ounces	29.57	milliliters	ml	milliliters	0.034	fluid ounces	fl oz
gal	gallons	3.785	liters	l	liters	0.264	gallons	gal
ft ³	cubic feet	0.028	meters cubed	m ³	meters cubed	35.71	cubic feet	ft ³
yd ³	cubic yards	0.765	meters cubed	m ³	meters cubed	1.307	cubic yards	yd ³
MASS								
oz	ounces	28.35	grams	g	grams	0.035	ounces	oz
lb	pounds	0.454	kilograms	kg	kilograms	2.202	pounds	lb
T	short tons (2000 lb)	0.907	megagrams	Mg	megagrams	1.103	short tons (2000 lb)	T
TEMPERATURE (exact)								
°F	Fahrenheit temperature	5(F-32)/9 or (F-32)/1.8	Celsius temperature	°C	Celsius temperature	1.8C + 32	Fahrenheit temperature	°F
ILLUMINATION								
fc	foot-candles	10.76	lux	lx	lux	0.0929	foot-candles	fc
fl	foot-Lamberts	3.426	candela/m ²	cd/m ²	candela/m ²	0.2919	foot-Lamberts	fl
FORCE and PRESSURE or STRESS								
lbf	poundforce	4.45	newtons	N	newtons	0.225	poundforce	lbf
psi	poundforce per square inch	6.89	kilopascals	kPa	kilopascals	0.145	poundforce per square inch	psi

NOTE: Volumes greater than 1000 l shall be shown in m³.

* SI is the symbol for the International System of Units

(Revised January 1992)

CONTENTS

Section	Page
EXECUTIVE SUMMARY -----	ES-1
1. INTRODUCTION -----	1
1.1 Heat Transfer Analysis -----	2
1.2 Beam Structural Analysis-----	2
1.3 Objectives -----	4
1.4 Accomplishments-----	5
2. THERMAL ANALYSIS -----	6
2.1 Design Codes -----	7
2.2 Finite Element Analysis-----	7
2.2.1 Material and Heat Transfer Properties -----	11
2.2.2 Environmental Conditions -----	14
2.3 Numerical Results and Parametric Studies -----	15
2.3.1 Horizontal Temperature Distribution-----	15
2.3.2 Vertical Temperature Distribution -----	17
2.3.3 Effects of Guideway Orientation and Season-----	20
2.3.4 Effects of Surface Treatments on the Guideway -----	23
2.3.5 Effects of Ground Radiation and Convection-----	27
2.3.6 Effects of Vehicle Induced Heating -----	35
2.4 Summary of Thermal Analysis -----	40
3. DEFLECTION AND STRESS ANALYSIS -----	43
3.1 Beam Theory-----	43
3.2 Finite Element Analysis-----	46
3.3 Numerical Results and Parametric Studies -----	46
3.3.1 Vertical Deflection-----	47
3.3.2 Horizontal Deflections-----	49
3.3.3 Effects of Guideway Orientation and Season-----	50
3.3.4 Effects of Surface Treatments on the Guideway -----	53
3.3.5 Effects of Ground Radiation and Convection-----	55
3.3.6 Effects of Vehicle Induced Heating -----	56
3.3.7 Double Spans versus Single Spans-----	57
3.3.8 Local Thermal Buckling Potential -----	60
3.3.9 Thermal Fatigue -----	64
3.4 Summary of Deflection/Stress Analysis -----	65
4. SAFETY IMPLICATIONS FOR THE TRANSPAPID MAGLEV GUIDEWAY -----	67
4.1 Thermal Deflections-----	67

Section	Page
4.2 Thermal Stresses -----	68
5. CONCLUSIONS AND RECOMMENDATIONS-----	69
5.1 Temperature Distribution -----	69
5.2 Thermal Deflections and Stresses -----	70
5.3 Recommendations-----	71
6. REFERENCES-----	72
APPENDIX A - COMPARISON TO OTHER TRANSPERID GUIDEWAY DESIGNS -----	A-1

ILLUSTRATIONS

Figure	Page
1-1 Transient Heat Transfer Analysis -----	3
1-2 Beam Structural Analysis -----	3
2-1 Directions for Guideway Parameters -----	6
2-2 Thermal Gradients Used in Design Codes -----	8
2-3 Heat Transfer in an Elevated Guideway -----	9
2-4 Schematic of Heat Transfer Conditions Used by FETAB -----	11
2-5 Typical Steel Guideway Design -----	12
2-6 Finite Element Model of the Steel Maglev Guideway Cross Section -----	12
2-7 Temperature Distribution Across Top Chord -----	16
2-8 Temperature Distribution Across Top Chord -----	18
2-9 Vertical Temperature Gradient, "Insulated" Case -----	19
2-10 Vertical Temperature Gradient, "Uninsulated" Case -----	19
2-11 Vertical Temperature Gradients throughout the Day -----	20
2-12 Temperature Distribution Across Top Chord -----	22
2-13 Vertical Temperature Gradient, Winter Conditions -----	23
2-14 Effect of Oxidized Steel on Transverse Top Chord Temperature Distribution -----	25
2-15 Effect of Oxidized Steel on Transverse Top Chord Temperature Distribution -----	26
2-16 Effect of Oxidized Steel on Temperature Gradient -----	27
2-17 Effect of Super-White Coating on Transverse Top Chord Temperature Distribution ---	28
2-18 Effect of Super-White Coating on Horizontal Temperature Distribution -----	29

Figure	Page
2-19	Effect of Super-White Coating on Temperature Gradient ----- 30
2-20	Effects of Surface Condition on Top Chord Lateral Temperature Distribution ----- 31
2-21	Guideway Heating from Ground Sources ----- 32
2-22	Thermal Model for Convection Between Ground and Guideway ----- 33
2-23	Effects of Ground Radiation/Convection on Vertical Temperature Gradient ----- 35
2-24	Transrapid Maglev Dissipated Power versus Frequency ----- 38
2-25	Transrapid Guideway Stator Pack Heating, Joule/meter ----- 39
3-1	Coordinate Reference ----- 44
3-2	Vertical Deflection versus Time of Day ----- 47
3-3	Horizontal Deflection versus Time of Day ----- 49
3-4	Effects of Guideway Orientation, Baseline Case, Summer Conditions ----- 50
3-5	Effects of Guideway Orientation ----- 51
3-6	Maximum Vertical Deflection versus Orientation and Time of Year ----- 52
3-7	Maximum Horizontal Deflection versus Orientation and Time of Year ----- 53
3-8	Effectiveness of Guideway Coatings in Reducing Thermal Deflections ----- 55
3-9	Effects of Ground Radiation/Convection on Vertical Deflections ----- 56
3-10	Thermal Deflection in Single and Double Span Guideways ----- 57
3-11	Deflection Comparison of Thermal and Static Live Loads for Double Span Guideway Configuration ----- 59
3-12	Slope Discontinuity Between Adjacent Guideway Beams ----- 59
3-13	Plate Buckling of Guideway Top Chord ----- 61
3-14	Generic Fatigue Data for A-36 Steel in Welded Construction ----- 64

TABLES

Table		Page
2-1	Material Properties for Guideway Analysis-----	13
2-2	Heat Transfer Properties for Guideway Analysis-----	13
2-3	Baseline Environmental Conditions for Guideway Analysis -----	14
2-4	Radiation Heat Transfer Properties for Various Surface Conditions-----	24
2-5	Effective Solar Absorptivity for Reflected Radiation on Bottom Chord-----	32
2-6	Heat Transfer to Bottom Chord by Direct Radiation and Convection from Ground ----	34
2-7	Typical Scenarios and Degrees of Freedom-----	36
2-8	Winding Temperature Rise per Vehicle Passage -----	40
3-1	Effects of Guideway Surface Treatment of Thermal Deflection -----	54
3-2	Summary of Stresses in Guideway Top Chord -----	63
3-3	Maximum Deflection Summary -----	66
4-1	Likely Significance of Vertical Thermal Deflections for Safety and Ride Quality -----	68

LIST OF SYMBOLS AND ABBREVIATIONS

a	plate length, or slot length
A	cross section area
b	plate width, or conductor width
c	specific heat capacity
D	guideway height above ground, or plate flexural rigidity
E	Young's modulus
F	view factor
h	heat transfer film coefficient
I	motor current
I_{xx}	section moment of inertia about x-axis
I_{yy}	section moment of inertia about y-axis
k	thermal conductivity, or numerical factor for plate buckling analysis
L	total beam length for single span
M_{Tx}	thermal bending moment about x-axis
M_{Ty}	thermal bending moment about y-axis
M_x	bending moment about x-axis
M_y	bending moment about y-axis
P	dissipated power
P_T	axial thrust due to thermal load
\dot{q}	heat generated in guideway per unit volume
T	temperature
t	time, or plate thickness
u	horizontal deflection
v	vertical deflection
x	horizontal coordinate on guideway cross section
y	vertical coordinate on guideway cross section
z	coordinate along longitudinal axis of guideway
α_T	coefficient of thermal expansion
α_S	solar absorptivity
δ	deflection
ϵ	surface emissivity
μ_0	permeability constant
ρ	mass density
σ	Stefan-Boltzman constant
σ_{CR}	critical buckling stress
σ_{ZZ}	axial stress

EXECUTIVE SUMMARY

A Maglev system currently proposed for Orlando, FL is based on the German Transrapid design, which uses an electromagnetic suspension (EMS) system for levitation. Because of the small levitation gap (≈ 8 to 10 mm) between the vehicle and guideway, and the tight gap tolerances required with this system, the Federal Railroad Administration (FRA), as part of its safety mission, has identified the need to assess the thermal deflections that can occur in the Transrapid guideway. These deflections may be significant, and their influence on safety and passenger ride comfort needs to be assessed.

In response to this need, this report presents a theoretical analysis of the temperature distributions and thermal deflections that may occur in the Transrapid guideway design when subjected to the Orlando thermal environment. The analysis is performed on a typical steel Maglev guideway similar to the design currently being proposed for use in the Florida system. The analysis can readily be extended to the actual Transrapid design to be used in Florida.

In this work, transient, finite element heat transfer analyses are used to calculate the temperatures on the guideway and resulting thermal deflections and stresses. The results of this study indicate that the depthwise temperature distribution in the guideway is steep and nonlinear. Also, significant temperature variation in the transverse direction occurs across the top surface of the guideway. The structural analysis shows that these temperature gradients can induce vertical deflections up to 13 mm for a 25m simply supported single span under worst case conditions. Horizontal deflections of up to 8 mm are also possible for single span construction. Parametric studies indicate that the vertical deflections reach the 10 to 11 mm range in summer when the guideway is oriented in the North-South direction with a maximum of 13 mm for the spring-fall equinoxes and an East-West orientation. Horizontal deflections are greatest in winter when the guideway is oriented in the East-West direction. These predicted deflections for the single span guideway will be used for comparison to the trends and results obtained from the planned test program, which will employ a full-scale single span girder for measurement of temperature distributions and thermal deflections. For revenue service conditions, however, the guideway beam will be used in a double span configuration. For the double span guideway (2 spans of 25m each), the results of this analysis indicate that the temperature gradients induce maximum vertical deflections of approximately 4 mm, and maximum horizontal deflections of approximately 2.5 mm, assuming full horizontal and vertical restraint at the center pylon.

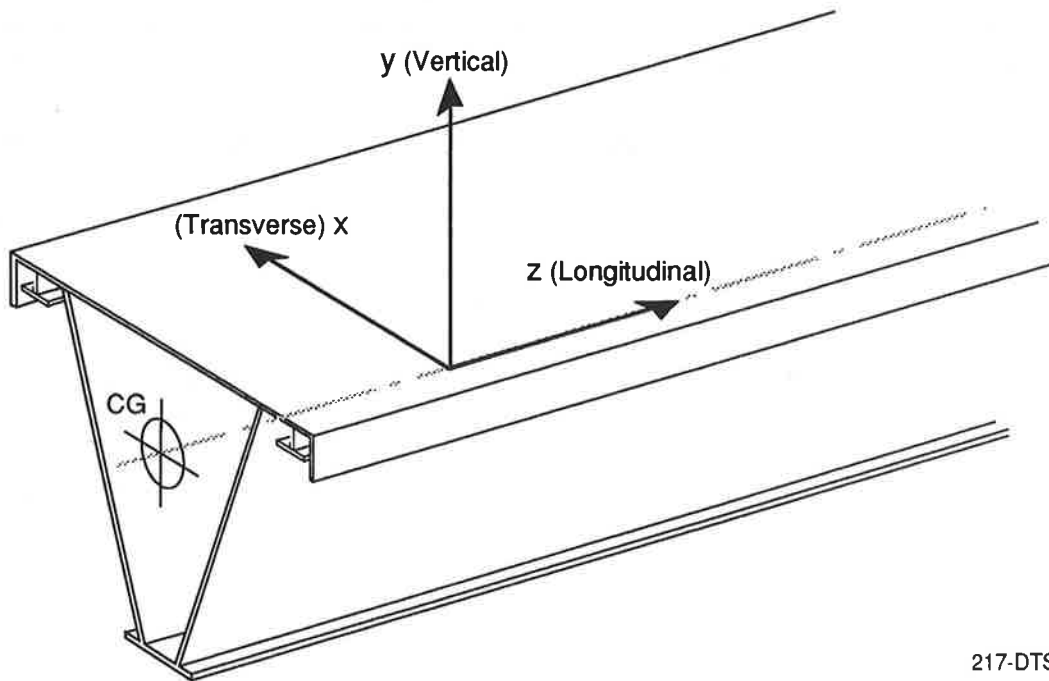
The parametric studies showed that the most important factors determining the thermal response are the sun angles (time of day, season and guideway orientation) and the thermal

2. THERMAL ANALYSIS

The temperature rise and distribution in a guideway structure can generate vertical and transverse deflections and bending moments as well as longitudinal movements and forces. Therefore, the determination of this temperature distribution is an important consideration in the analysis of the structural response.

For reference, the directions used in this report for guideway parameters are shown in Figure 2-1.

Methods suitable to the determination of the temperature distribution in the structure are: (1) design codes; and (2) analytical or finite element techniques. These methods, and their application to the thermal analysis of the guideway beam are described in the following subsections. Design codes were surveyed first to evaluate their appropriateness and accuracy for determining the thermal beam response.



217-DTS-9612-8

Figure 2-1. Directions for Guideway Parameters

2.1 Design Codes

Several countries have formulated design codes to give the depthwise temperature distribution in elevated guideways. In the codes, the temperature distribution is generally assumed to be uniform both in the transverse direction of the beam cross section, and along the longitudinal axis of the beam. A summary of the codes employed by various countries, including New Zealand, England, Australia and France is shown in Figure 2-2 (3). The New Zealand code is generally the most severe, having the steepest gradient and the highest maximum temperatures, and is considered by many researchers to be the most useful code for guideways in the U.S. thermal environment. The other codes, in contrast, are considered to be less adequate, since they are too simplistic (such as the linear French code), or have maximum temperatures which are too low for the temperature extremes encountered in the United States. However, even the New Zealand code has shortcomings, especially in its application to the Transrapid Florida guideway. These include:

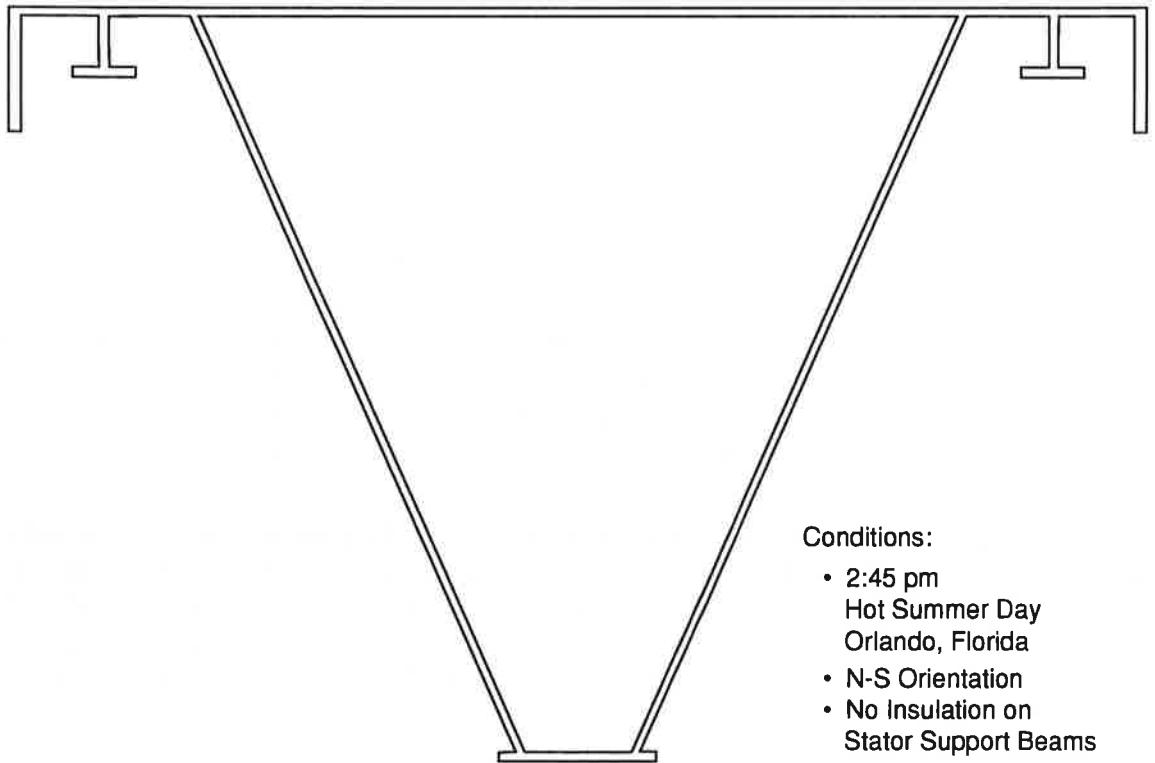
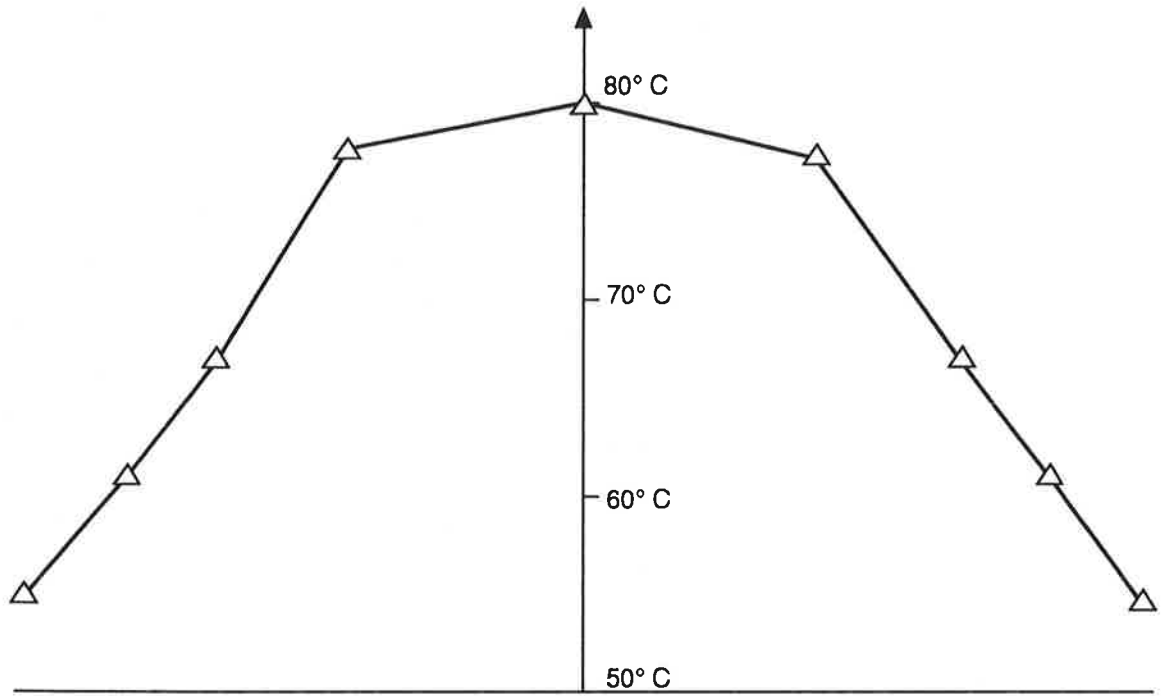
- As with the other design codes, the New Zealand code was developed for concrete, thick-walled box-girder bridges which are typically used in highway applications. The code has not been experimentally validated for the Transrapid steel Maglev guideway to be erected in Florida.
- The code does not account for the “reversed” depthwise temperature gradient which can result from the guideway cooling at night. In such a case, the bottom portions of the guideway will be hotter than the top flange, resulting in downward deflection of the guideway.
- The code also does not account for transverse temperature variations in the beam cross section. These temperature variations may be significant for the Transrapid Maglev guideway. Laterally symmetric variations change the effective average temperature at any given depth. Unsymmetric variations will induce lateral or horizontal deflections.

Existing codes may thus be of very limited use for detailed analysis of guideway thermal response. A more accurate and rigorous approach to calculate the actual temperature distribution and evaluate deflections for the guideway will be required.

2.2 Finite Element Analysis

The modes of heat transfer in the elevated guideway structure are shown schematically in Figure 2-3. The input heat is due to incident solar or ground-reflected radiation. In some cases, vehicle induced heating may also be a factor. The heat loss consists of long wave radiation and convection to the environment. The differential equation for the unsteady state heat transfer on the cross section is:

$$k \frac{\partial^2 T}{\partial x^2} + k \frac{\partial^2 T}{\partial y^2} + \dot{q} = \rho c \frac{\partial T}{\partial t} \quad (2-1)$$



- Conditions:
- 2:45 pm
 - Hot Summer Day
 - Orlando, Florida
 - N-S Orientation
 - No Insulation on Stator Support Beams

218-DTS-9612-2

Figure 2-7. Temperature Distribution Across Top Chord

Table 2-6. Heat Transfer to Bottom Chord by Direct Radiation and Convection from Ground

Guideway Height Above Ground, D (m)	q _R (W/m ²)	q _C (W/m ²)	Net Direct Heat Flux (q _R + q _C) (W/m ²)
1	25.0	33.9	58.9
2	6.30	33.9	40.2
5	2.20	33.9	36.1

simplicity, the convection heat transfer is assumed to be constant. This assumption is conservative, since the convection heat transfer will actually decrease with increasing height of the guideway above the ground level. The convection heat transfer will also vary throughout the day, but will be greatest for the night condition, as described above.

Finite Element Analysis of Ground Radiation and Convection Effects

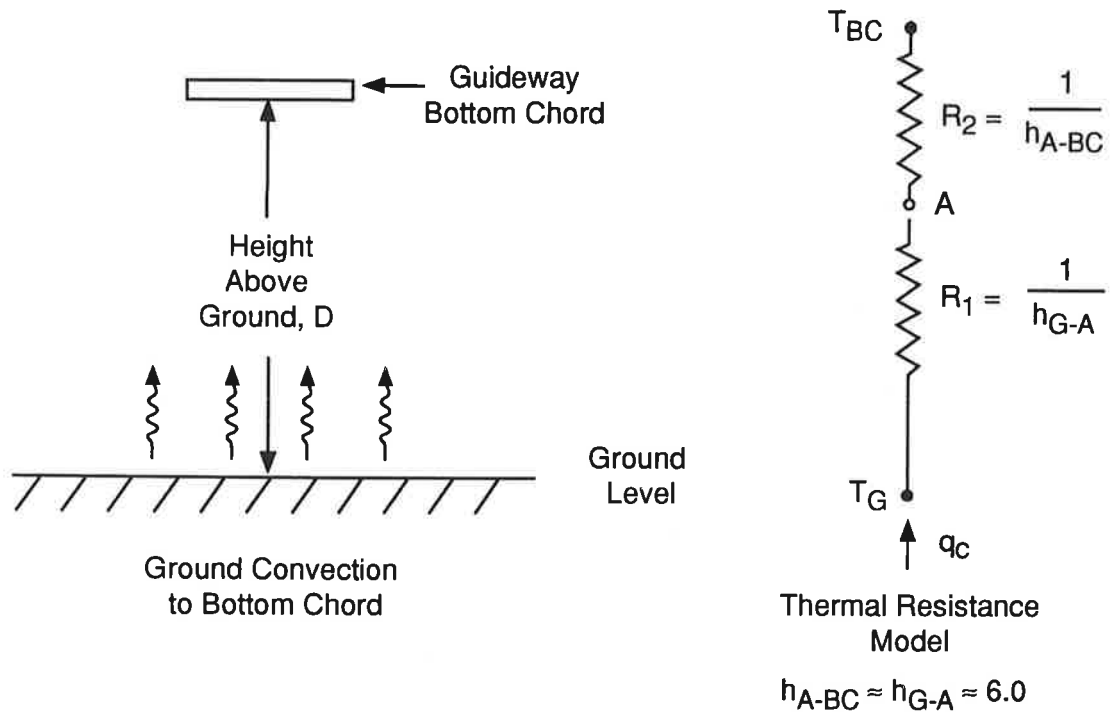
To quantify the effects of ground radiation and convection on the guideway temperature distribution, a parametric study was conducted with the finite element model. The model was modified to incorporate the bottom chord heating effects described above. The reflected radiation effects in daytime were incorporated using the effective bottom chord solar absorptivity, as listed in Table 2-5. The direct ground radiation and convection heat transfer effects (from Table 2-6) were taken into account by applying heat generation to the elements in the bottom chord of the finite element model. Assuming that the heat transferred by direct radiation and convection is absorbed uniformly in the bottom chord of the guideway, then the effective heat generation in the elements of the bottom chord is given by:

$$\dot{q}_{BC} = \frac{q_C + q_R}{t_{BC}}$$

where:

- \dot{q}_{BC} = heat generated per unit volume of the bottom chord
- t_{BC} = thickness of the bottom chord

These effects were incorporated into the model and the transient temperature distributions were calculated for the hot summer day conditions for several guideway heights above the ground surface. In each case, insulated stator support beams were assumed. The resulting temperature gradients through the guideway depth are shown in Figure 2-23. Note that the ground heating effects cause the temperatures in the bottom chord area to increase, forming a gradient in the lower portion of the guideway. As might be expected, these effects diminish as



187-DTS-9612-2

Figure 2-22. Thermal Model for Convection Between Ground and Guideway

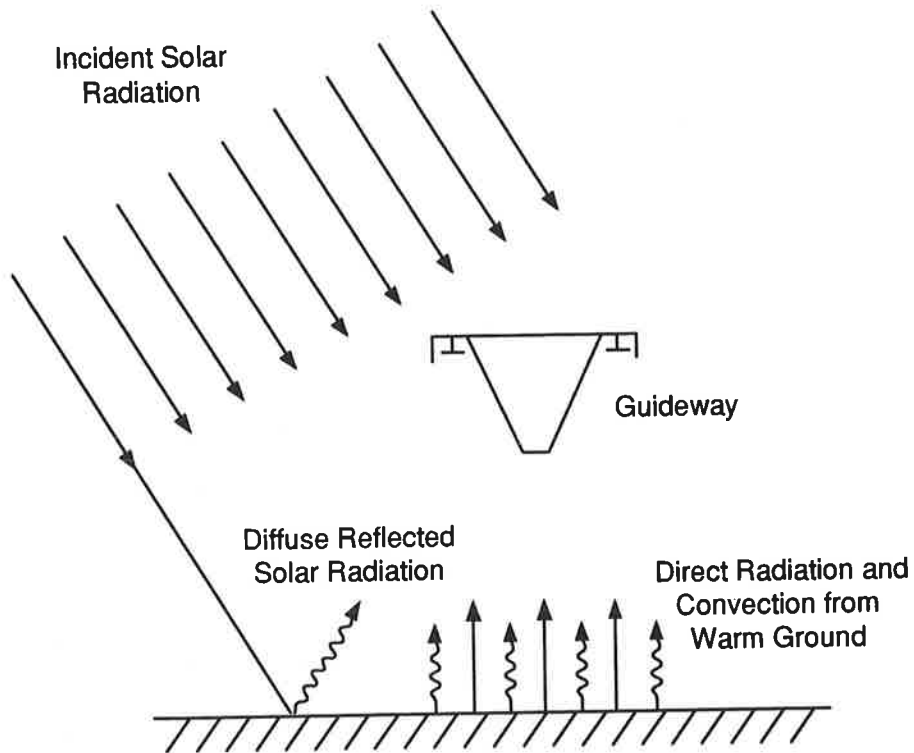
The additional heat transferred to the guideway by direct radiation from the ground was estimated using the equation:

$$q_R = \alpha_{LW} \sigma (T_G^4 - T_{BC}^4) F$$

where:

- q_R = heat transferred by direct radiation per unit area
- σ = Stefan-Boltzman constant ($5.669 \times 10^{-8} \text{ W/m}^2\text{-deg K}^4$)
- α_{LW} = guideway long-wave absorptivity
- F = view factor, as described above

As noted previously, the view factor accounts for geometrical effects, including the guideway height above the ground surface. The heat transferred to the bottom chord by direct radiation is thus a function of the guideway height above the ground. This effect is shown in Table 2-6, which lists the calculated heat flux to the guideway lower by direct ground radiation and convection for several guideway heights above the ground surface. Note that as the guideway height increases, the view factor and the direct radiation heat transfer both decrease sharply. For



187-DTS-9612-1

Figure 2-21. Guideway Heating from Ground Sources

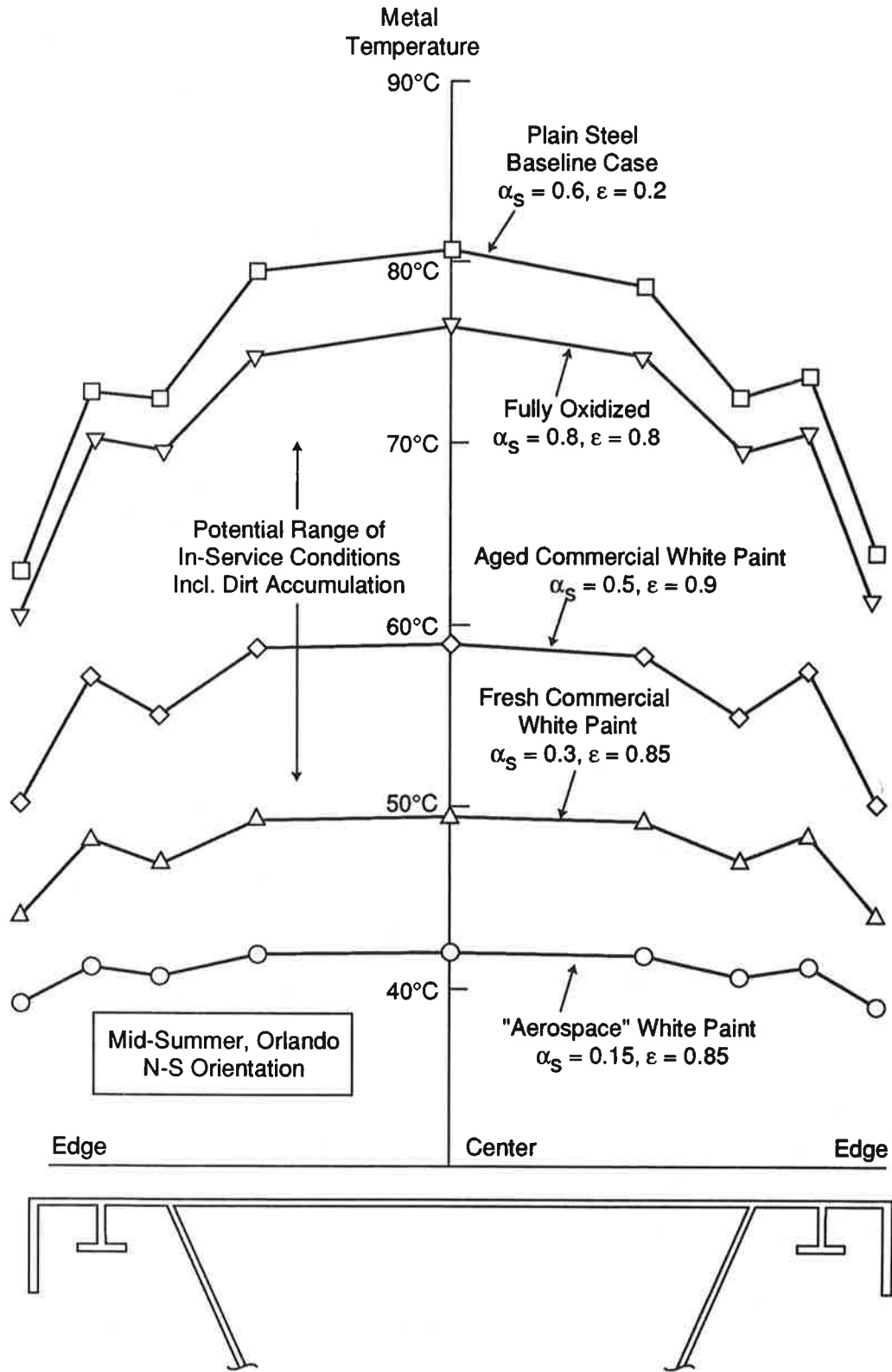
Table 2-5. Effective Solar Absorptivity for Reflected Radiation on Bottom Chord

Guideway Height Above Ground, D (m)	View Factor, F	Effective Bottom Chord Solar Absorptivity, α_{eff}
1	0.400	0.12
2	0.100	0.03
5	0.035	0.01

where:

- T_G = assumed ground temperature
- T_{BC} = guideway bottom chord temperature
- q_c = heat transferred by convection per unit area
- h_{G-A} = heat transfer film coefficient between the ground and the air
- h_{A-BC} = heat transfer file coefficient between the air and the bottom chord

For the case in which the guideway temperature at night is approximately 26.7°C (80°F) and the ground temperature is assumed constant at 38°C (100°F), the amount of heat transferred by convection between the ground and the guideway bottom chord was calculated to be approximately 33.9 W/m².



218-DTS-9612-23

Figure 2-20. Effects of Surface Condition on Top Chord Lateral Temperature Distribution

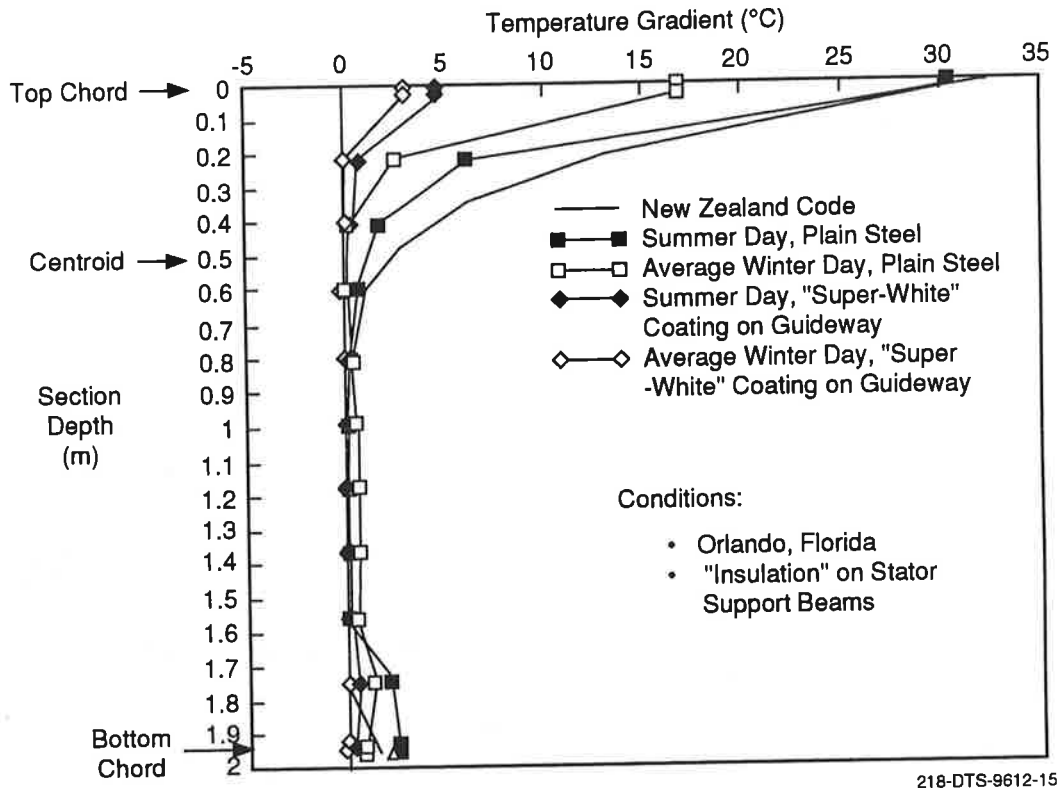


Figure 2-19. Effect of Super-White Coating on Temperature Gradient

be particularly significant during the proposed guideway test program, since the guideway will be mounted close to ground level on relatively short pylons. The close proximity of the guideway to the ground and the high heat capacity of the concrete ground surface may be expected to increase the amount of heat transferred from the ground to the lower portion of the guideway.

To model the direct ground radiation and convection effects, the amount of heat transferred between the ground and the guideway was estimated as follows. During the night, the temperature of the guideway is approximately that of the ambient air, while the ground surface can be assumed to maintain a roughly constant temperature. The heat transfer by convection between the ground and the bottom chord was calculated using a one-dimensional thermal resistance model, as shown in Figure 2-22. The warm ground in this model heats the air above it, and this heat is then transferred by convection to the guideway. The amount of heat transferred is calculated from:

$$q_c = \frac{(T_G - T_{BC})}{\left(\frac{1}{h_{A-BC}} + \frac{1}{h_{G-A}} \right)}$$

of the day. Due to the lack of direct sunlight, the temperatures of the side rails and webs are reduced, and the difference in temperature between the two webs is small.

The top chord, however, is not subject to these shade effects. The temperature variations on the top chord (20 to 25°C from the hottest point at the center to the side rails, as noted above) are still present, regardless of the guideway orientation.

Seasonal Variations

A study similar to the above was performed for winter conditions. For this study, average winter day conditions for Orlando were used, with ambient temperatures of $T_{\max} = 22.8^{\circ}\text{C}$ (73°F) and $T_{\min} = 10.6^{\circ}\text{C}$ (51°F). In addition to the lower ambient temperatures, the amount of solar radiation incident on the guideway in winter is greatly reduced in comparison to summer.

The FE model shows that the winter conditions affect both the horizontal and vertical temperature distributions. The horizontal distributions across the top chord for winter and summer conditions for a N-S orientation are compared in Figure 2-12. The winter temperatures are reduced in comparison to the summer conditions. The temperature differential between the center of the top chord and the side rails is also slightly reduced. However, during the early morning and late afternoon hours, the temperature differential between the main webs (one in direct sunlight, the other in shade) is approximately 20 to 25°C, which is greater than the difference occurring in the summer.

The effects of winter conditions are even more noticeable in the vertical temperature gradient, as illustrated by Figure 2-13 for the “insulated” case. Here the top chord temperatures are less than 20°C hotter than the average web temperatures. The gradient in the winter conditions is much less severe than the gradient in summer, or the predictions of the New Zealand code. This reduced gradient will also result in smaller vertical deflections in winter, as discussed in the following sections.

Survey of Combined Effects of Orientation and Season

Further studies with the heat transfer model indicated that the magnitude of the maximum daily transient thermal gradients were affected by the individual combination of orientation and season. In retrospect, this seems reasonable since both determine the angle of solar incidence on the guideway in three-dimensional space, which in turn directly relates to heat input. Therefore, combinations of guideway orientations from N-S to E-W with different seasonal points were made. The results are fully discussed later in subsection 3.3.3 describing the deflection response, but it was found that the E-W orientation in combination with the equinoxes produced slightly higher vertical gradients than the baseline “summer solstice/N-S” case, and that the E-W direction in combination with the mid-winter point produced the highest horizontal gradients. The full orientation range was explored for the equinoxes (March 21 and September 21), and the halfway points between summer solstice and equinox were checked for N-S and E-W (these latter were very close to the results for the solstice). In the interest of clarity, however, the baseline condition can be used for these discussions of parametric influences.

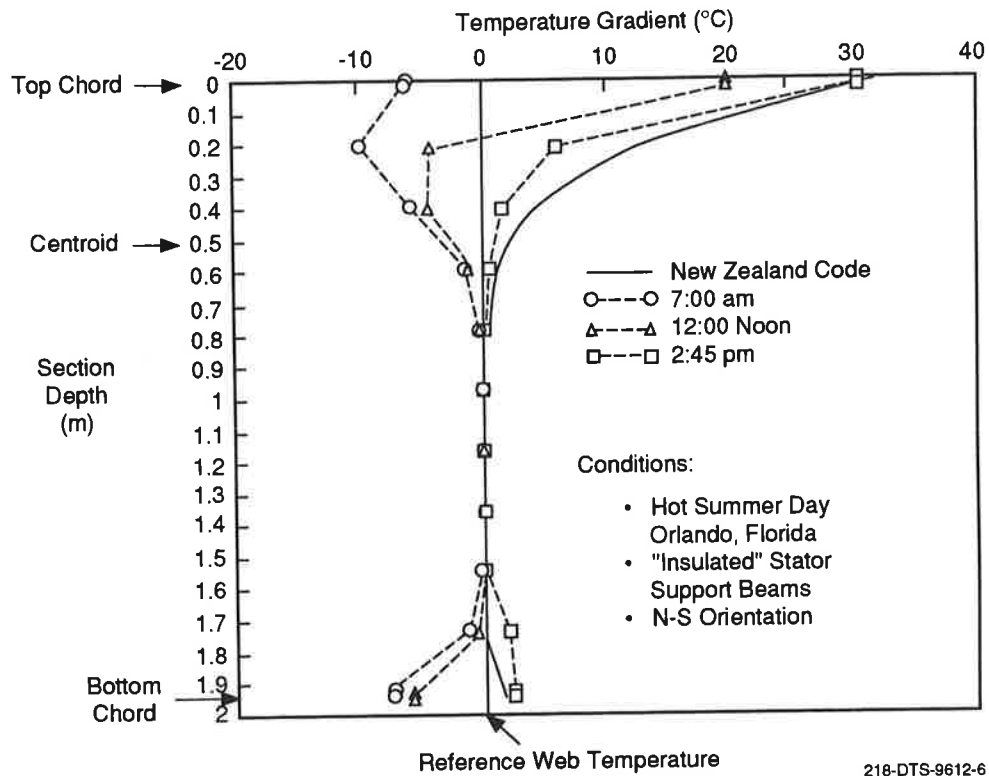


Figure 2-11. Vertical Temperature Gradients throughout the Day ("Insulated" Case)

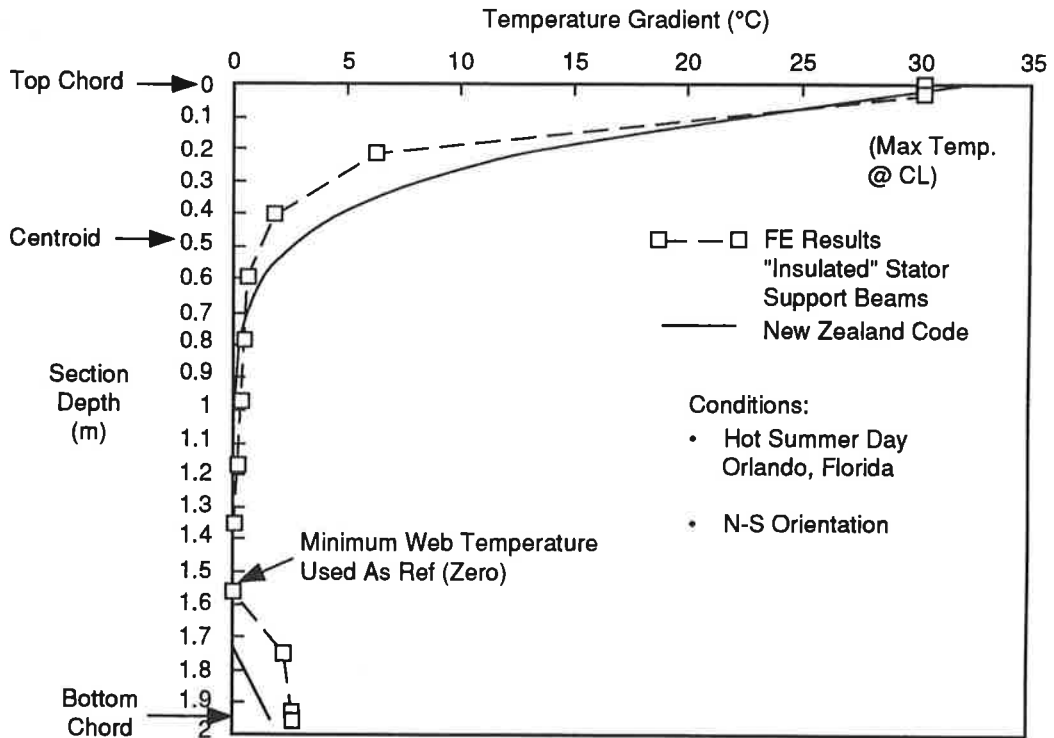
It must be noted again here that the New Zealand code assumes the top chord to be at uniform temperature. Thus, although the code is reasonable for the prediction of the maximum vertical temperature gradient, it cannot predict the variation of temperature across the top chord, nor can it be used to predict the variations in temperature gradient throughout the day. Consequently, beam deflections and stresses based on code assumptions can differ from those calculated with the actual distribution of temperatures across the section. Note that, however, use of the centerline top chord temperature as a temperature for the full top chord would overestimate the thermal moment. The true thermal moment must use the actual thermal distribution.

2.3.3 Effects of Guideway Orientation and Season

Guideway Orientation

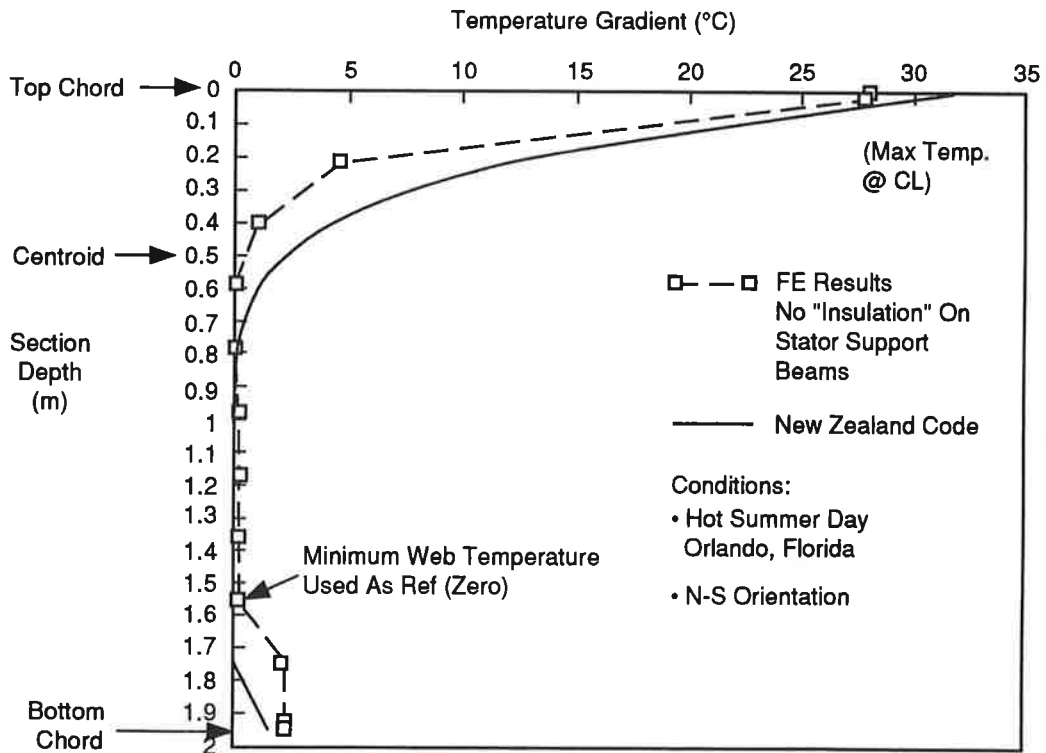
The effects of guideway orientation (compass direction) on the guideway temperature distribution were also studied using the FE model. The orientation primarily affects the horizontal temperature distribution. When the guideway is oriented in the North-South direction, large horizontal temperature gradients occur, due to the sun's heating of one of the webs while the other is in shade. As described above, these effects can result in the heated web being 15 to 20°C hotter than the shaded web.

When the guideway is oriented in the East-West direction in summer conditions, the web heating effects are reduced, since both webs are in the shadow cast by the upper chord for most



218-DTS-9612-3

Figure 2-9. Vertical Temperature Gradient, "Insulated" Case (with Stator Packs)



218-DTS-9612-4

Figure 2-10. Vertical Temperature Gradient, "Uninsulated" Case (Bare Guideway)

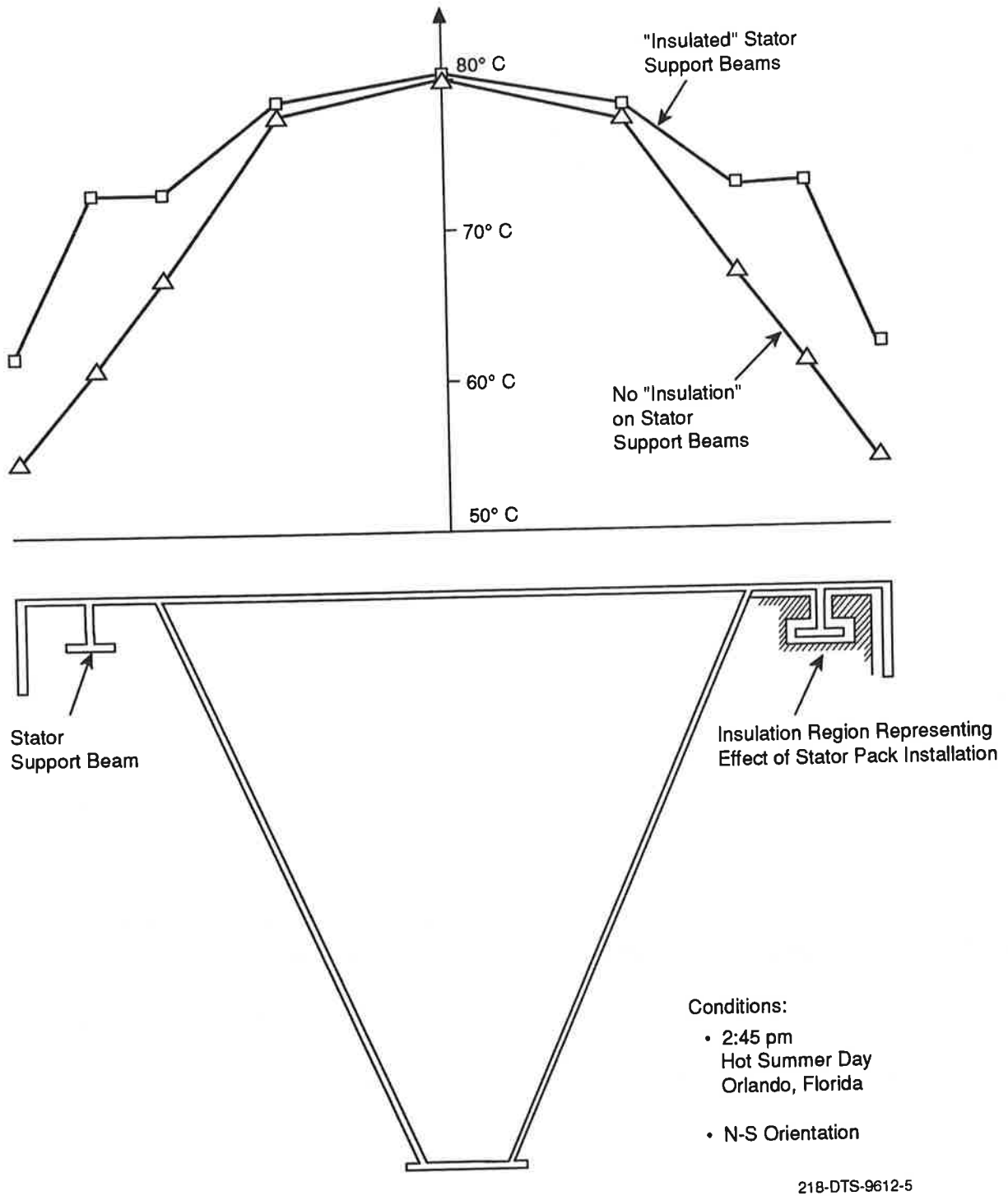


Figure 2-8. Temperature Distribution Across Top Chord (Insulated and Uninsulated Cases)

of the high amount of solar energy incident on the thin steel structure of the top chord of the Florida guideway, the temperature results of the finite element model are believed to be reasonable for a worst case assessment of temperature and deflection, assuming the guideway has no reflective surface treatments, such as white paint.

During early morning or late afternoon hours when the sun is low in the sky, the results also show that significant unsymmetrical lateral temperature gradients occur in the guideway. The web on the sunny side can be 15 to 20°C hotter than the shaded side web. Again, these effects, due to the daily variation in the sun's position, are not accounted for in the design codes. These transverse temperature variations are important, since they will induce large lateral deflections, as calculated in the next section.

The effects of equipment attached to the guideway may also be significant. For example, when stator packs or other equipment are attached to the underside of the stator support beams, then this portion of the guideway may have reduced convection and radiation to the environment, and may thus be effectively insulated. These effects were bracketed by insulating the region around the stator support beams, as shown in Figure 2-8. The effects of this insulation are also shown on the figure, which compares the temperature distributions across the top chord for the insulated and uninsulated cases. The temperatures on the top chord of the uninsulated case rapidly decrease near the side rails, due to the large surface area of the rails and stator support beams, which transfer heat to the environment. In the insulated case, less heat is transferred due to the insulating effects of the guideway equipment and the temperature gradients across the top chord are reduced.

2.3.2 Vertical Temperature Distribution

For the hot summer day conditions in Orlando, the FE model gives a vertical temperature gradient similar to the New Zealand code. The results show that the vertical temperature gradient through the webs to the top chord is steep and nonlinear. This is shown in Figures 2-9 and 2-10 which compare the calculated temperature gradients for the insulated and uninsulated cases. At the hottest (CL) point on the top chord, the FE model predicts a temperature which is 28 to 30°C hotter than the minimum web temperature. This agrees well with the New Zealand code, which predicts the top chord to be 32°C hotter than the minimum web temperature. In these figures, the web temperatures shown reflect the average of the left and right webs, while the upper chord temperatures correspond to the center of the top flange.

As the sun's position and the ambient temperature change throughout the day, the guideway temperature distribution and gradient will change as well. The results of the transient heat transfer analysis are illustrated in Figure 2-11 which shows the vertical temperature gradient at three different times during the day: 7:00 a.m., 12:00 noon, and 2:45 p.m. Note that at 7:00 a.m., the average web temperature is warmer than the top and bottom chords of the guideway, since the sun is low in the sky, and is directly heating one web. Later in the day, at noon, the sun is directly overhead, and is directly heating the top chord. By mid afternoon, the entire upper portion of the guideway has been heated by the sun, resulting in the steep gradient similar to the New Zealand code.

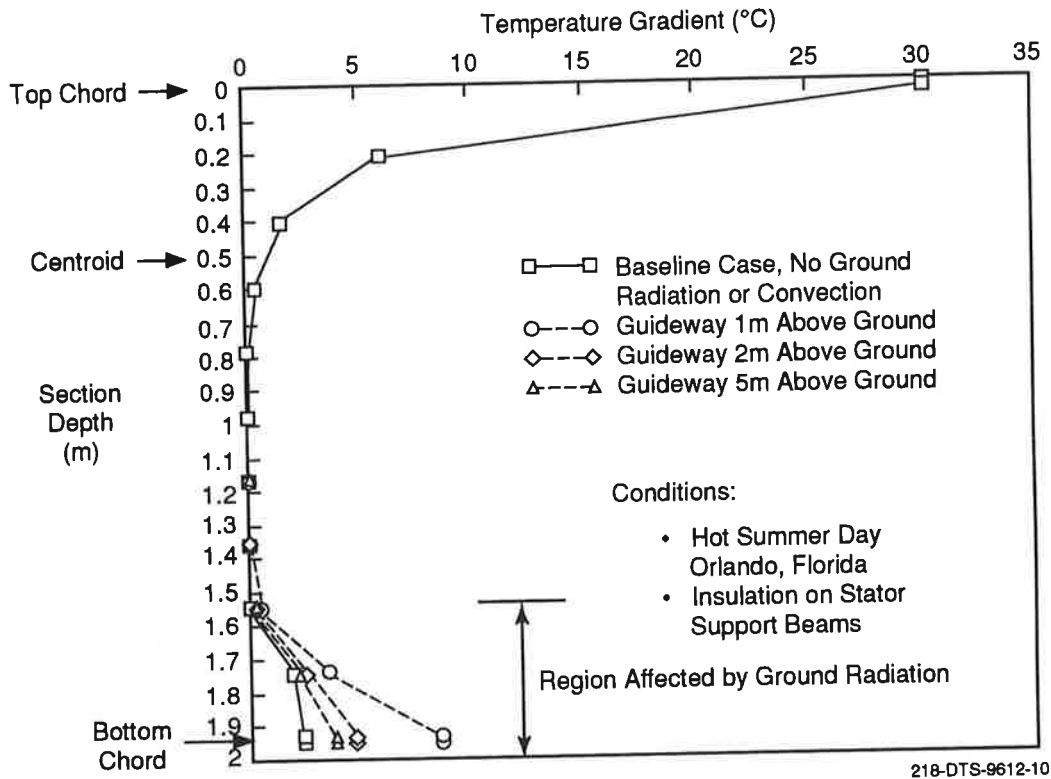


Figure 2-23. Effects of Ground Radiation/Convection on Vertical Temperature Gradient

the guideway height above the ground level increases. In the upper portion of the guideway, the temperatures are essentially unchanged from the baseline case, which does not include ground radiation or convection effects. The ground radiation primarily affects the lower chord plate, due to rapid fall-off of the thermal effects with distance (height above ground). If the lower chord plate changes significantly in width in further designs, this effect could be accounted for via this analysis approach.

2.3.6 Effects of Vehicle Induced Heating

In addition to solar and ground radiation/convection heating, the guideway is also subject to heating from the vehicle. As the vehicle passes, resistance losses are generated in the windings and iron of the stator pack. These losses are dissipated as heat in the stator pack which can then heat the upper portion of the guideway.

Fundamentally there are two loss mechanisms: electrical resistive heating and magnetic hysteretic losses. The resistive losses are subdivided into ohmic losses in the stator winding, eddy current losses in the winding, and eddy losses in the iron stator pack. The resistive losses are the greatest, and are discussed below.

The two primary operational factors which determine these power losses are the motor thrust and vehicle speed. Table 2-7 shows thrust and speed for several scenarios (accelerate, cruise,

where:

- L_v = length of field imposed by the vehicle
- η_{Fe} = resistivity of iron
- B = peak magnetic field at the stator pack
- t = iron lamination thickness

Figure 2-24 shows the calculated Transrapid dissipated power versus frequency or vehicle speed. The results for the maximum and typical currents are indicated. (Note that the current is assumed to be a constant as a function of speed.) Eddy current and estimated hysteretic losses are also shown in the figure. (The winding eddy current losses are neglected since cable data was not available.) A curve showing the total resistive + iron eddy currents + iron hysteretic losses is also indicated. As the vehicle speed increases, the greater vehicle passing frequency increases losses.

Figure 2-25 shows the calculated Transrapid guideway stator pack heating versus frequency or vehicle speed. Again, data for two constant motor currents and the hysteretic losses and iron eddy losses are shown. This figure shows that for constant block lengths more energy is deposited at low speed in each meter of guideway even though less total power is dissipated. This occurs because the vehicle travels more slowly, increasing the length of time for dissipated energy to accumulate at a particular location along the guideway.

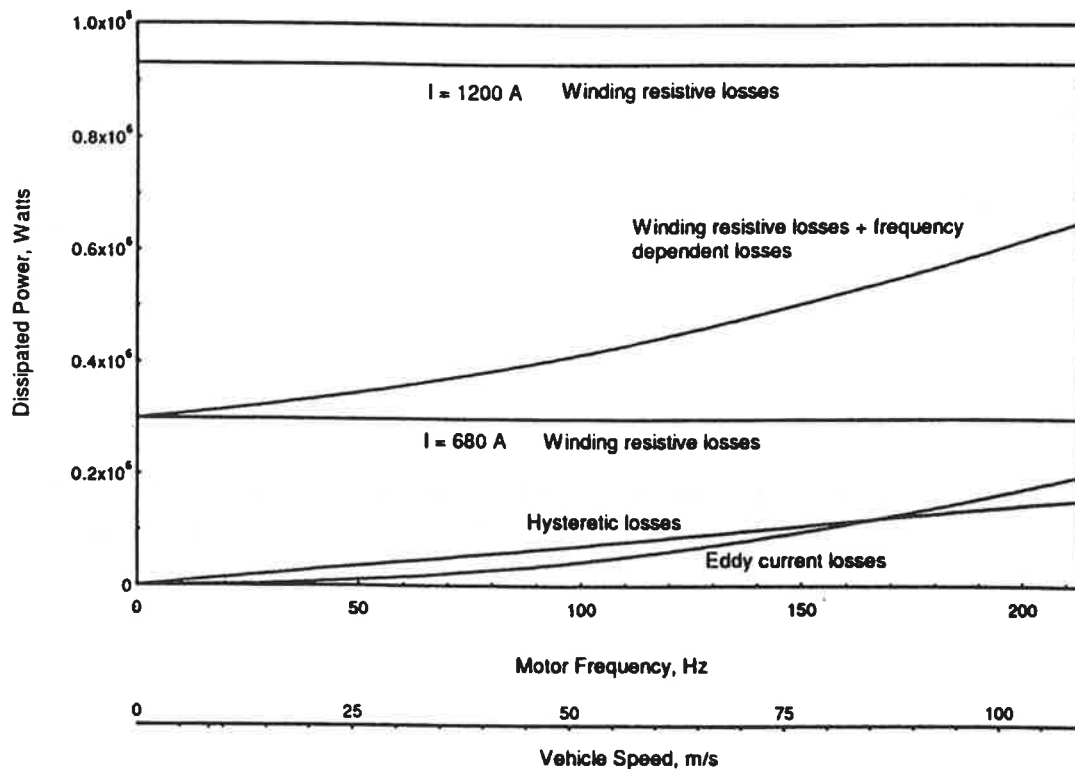


Figure 2-24. Transrapid Maglev Dissipated Power versus Frequency

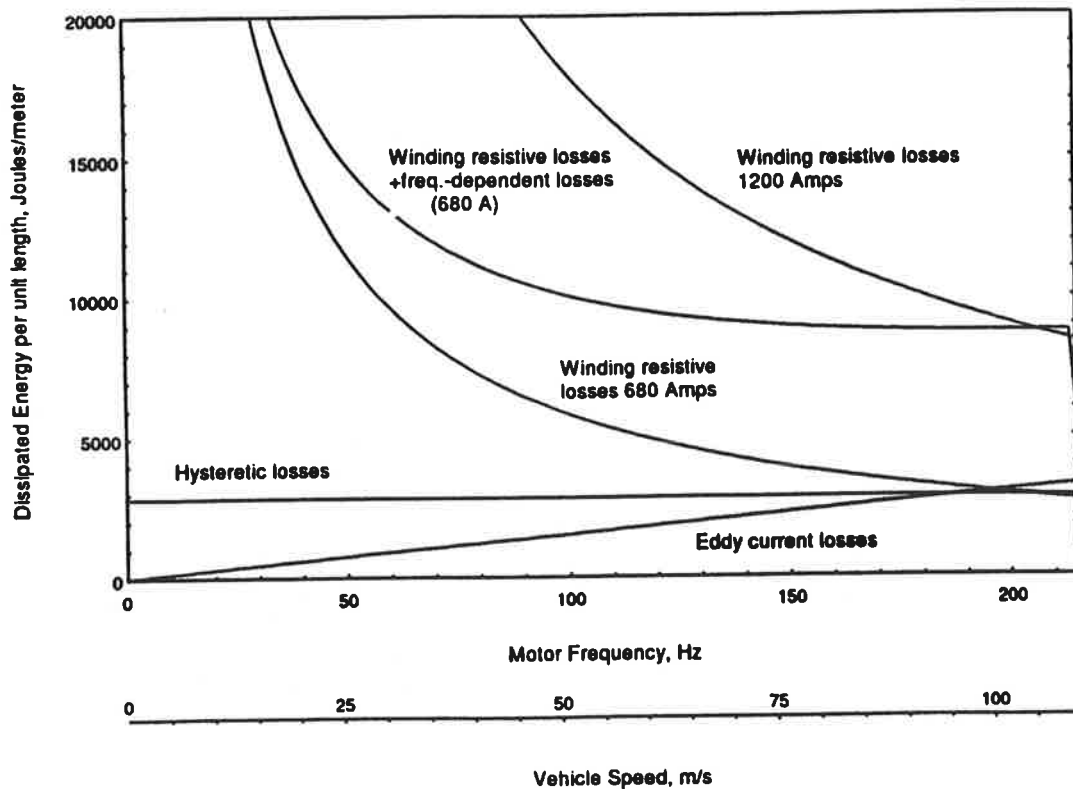


Figure 2-25. Transrapid Guideway Stator Pack Heating, Joule/meter

Table 2-8 shows the results of an adiabatic temperature rise in the windings due to a passing vehicle at two speeds and two values of motor thrust (current). This calculation only accounts for the ohmic losses in the motor windings due to the thrust-producing current. As expected, the temperature rise is greatest for low speed, high thrust scenarios.

These results show that the resistive losses in the stator packs due to vehicle passage may induce significant heating in the stator windings. A more accurate quantitative assessment of these heating effects requires more detailed knowledge of the stator pack design, and is beyond the scope of this study. However, the results of this analysis do indicate that vehicle induced heating effects should be considered in the analysis of guideway temperatures and thermal deflections found in revenue service conditions.

Effects on Stator Pack and Guideway Temperatures

As noted above, the power losses are dissipated as heat, primarily in the windings and iron of the stator pack. The results listed in Table 2-8 show that *a single pass of a vehicle* at low speed can increase the temperature of the stator pack windings by 3.1°C (5.6°F). For a series of vehicles traveling at short headway, the temperature rise in the stator windings will be considerably larger.

Table 2-8. Winding Temperature Rise per Vehicle Passage

Speed (m/sec)	Current, Amps (thrust)	Energy Deposited per Distance (J/m)	ΔT ($^{\circ}C$)
55	680	5,350	1.0
	1,200	16,700	3.1
110	680	2,600	0.5
	1,200	8,300	1.6

Since the stator packs are mounted in the upper portion of the guideway on the stator support beams, it can be assumed that the heat from the stator packs will partially transfer to the guideway structure, thereby increasing the temperatures in the upper portion of the guideway. However, quantification of these effects on the guideway temperatures requires knowledge of several detailed design features of the stator packs and guideway, including:

- The amount and effectiveness of the insulation surrounding the stator pack windings.
- Accurate sizing of the stator windings and core iron, with their thermal properties.
- How the stator packs are attached to the guideway, including the number and size of the bolted connections to the stator support beams.

On a qualitative basis, however, it can be stated that the heating of the stator windings due to vehicle passage can be significant, especially for a series of vehicles traveling at slow speed, such as at or near a station. Due to the proximity of the stator coils to the upper portion of the guideway, the guideway temperatures in this region can be expected to increase from the vehicle induced heating of the stator packs. These effects warrant further investigation and verification by testing in future work.

2.4 Summary of Thermal Analysis

The principal results for the thermal analysis of the Florida Maglev guideway beam are summarized below.

- Comparison of the FE heat transfer analysis with existing worldwide bridge design codes and practices showed that, for the steel TR guideway, these codes cannot fully reflect the thermal response sufficiently to assess both vertical and horizontal effects.
- The New Zealand design code has the most severe vertical temperature gradient of any of the commonly used codes, and is often recommended by researchers for use in the U.S. thermal environment. However, the design codes may be of limited use for detailed

analysis of Maglev guideways, since they do not account for horizontal temperature variations on the guideway cross section, nor are they convenient for assessing environmental and location factors affecting thermal distributions.

- Results from the FE analysis have shown that the vertical temperature distribution in the Transrapid guideway under hot summer day conditions agrees reasonably well with the predictions of the fifth order New Zealand code. The FE model predicts that the temperature differential between the hottest point on the top chord and the coldest point on the web is 28 to 30°C. The New Zealand code is slightly more conservative, and predicts a temperature differential of 32°C.
- The FE model shows that the transverse variations in temperature can be significant. On the top chord of the guideway the temperature of the side rails can be as much as 20 to 25°C lower than the center of the top chord. These effects are caused by the large surface area of the side rails and stator support beams, which readily transfer heat from the guideway to the environment. These effects are not accounted for in the design codes, which all assume that the top chord is uniform in temperature, with no horizontal temperature variation in the structure.
- The presence of guideway mounted equipment (such as stator packs) affects the top chord temperatures. This equipment reduces the temperature variation across the top chord, thereby raising average top chord temperature. Test configurations need to include effects of stator packs to evaluate deployed guideways.
- During the early morning and late afternoon hours, the temperature differential between the main webs can be 15 to 25°C, due to direct solar heating of one of the webs while the other is in shade. These effects are not predicted by the design codes, and are considered to be important in the evaluation of lateral deflection.
- Guideway orientation (compass direction) seems to primarily affect the horizontal temperature distribution. However, certain combinations of orientation (E-W) and season (equinoxes) can produce vertical gradients somewhat higher than the summer/N-S baseline case.
- Seasonal variations affect both the vertical and horizontal temperature distributions. The guideway temperatures and vertical temperature gradient are reduced in winter. However, during the early morning or late afternoon hours, the temperature differential between the heated and shaded webs in winter is greater than occurs in summer.
- Ambient air temperatures are much less influential than the effects of orientation, location and season.
- The surface treatment of the guideway can strongly affect the temperature distribution in the guideway. The temperatures and temperature gradients in an oxidized steel guideway are slightly reduced in comparison to the baseline untreated steel guideway. Both plain

steel and oxidized surfaces tend to the worst-case (highest gradients and temperatures) compared to a coated guideway.

- Adding white paint to all guideway surfaces sharply reduces the guideway temperatures and temperature gradients in both summer and winter. The type and condition of the paint significantly affects the reductions that can be obtained.
- Ground radiation and convection to the guideway can increase temperature somewhat in the lower portion of the guideway. The effect is greatest when the guideway is mounted close to the ground on short pylons, and can increase temperatures in the bottom chord by about 5°C during the day.
- Eddy current and resistive power losses from passing or stationary vehicle passage are dissipated in the stator packs as heat. Slower, frequent, and stationary vehicles increase these effects. The temperature increase in the stator packs can be significant, especially near Maglev stations. These effects may increase the temperatures in the upper portion of the guideway, and need further investigation, especially for the levitation power losses which are expected to be significant.

3. DEFLECTION AND STRESS ANALYSIS

Once the temperature distribution in the guideway is known, the structure can be analyzed using beam theory to determine the thermal vertical and horizontal deflections, and the thermal bending stresses. The subsections below present the relevant aspects of beam theory, and detail the deflection and stress analysis results obtained for the Transrapid Maglev guideway beam. Several parametric studies are presented to determine the scenarios for maximum vertical and horizontal deflection.

The deflection results and parametric studies are presented first for the single span conditions. This will allow for direct comparison of these results of an upcoming test program, which will measure the thermal deflections of the guideway beam while mounted in a single span configuration. However, it is anticipated that the guideway used in the Orlando, FL Maglev system will employ a double span configuration. A later subsection of this report will thus detail the deflection analysis and results pertaining to the guideway when installed in a double span configuration, which reduces deflections significantly, while increasing stresses.

3.1 Beam Theory

We follow the beam theory equations given in Boley (10), with sign conventions as shown in Figure 3-1. Under the assumption that plane cross sections remain plane after deformation, it can be shown that the longitudinal displacement and strain at any cross section are:

$$w = f_0 + f_1 y + f_2 x \quad (3-1)$$

$$e_{zz} = \frac{\partial w}{\partial z} = f'_0 + f'_1 y + f'_2 x \quad (3-2)$$

with the standard nomenclature:

- x = horizontal (transverse) coordinate on cross section
- y = vertical coordinate on cross section
- z = longitudinal coordinate
- w = longitudinal displacement in z-direction
- e_{zz} = longitudinal mechanical strain
- f_0, f_1, f_2 = functions of z (longitudinal coordinate)
- f'_0, f'_1, f'_2 = derivatives with respect to z

$$EI_{xx} \frac{d^2v}{dz^2} = -(M_{Tx} + M_x) \quad (3-11)$$

$$EI_{yy} \frac{d^2u}{dz^2} = -(M_{Ty} + M_y) \quad (3-12)$$

where

- u = horizontal (transverse) displacement in x direction
- v = vertical displacement in y direction
- M_x, M_y = bending moments due to applied loads or constraints

At $z = 0$ and $z = L$, (the beam ends), the boundary conditions require that the horizontal and vertical displacements are zero:

$$u = v = 0$$

Assuming the temperature distributions and thermal moments to be uniform along the longitudinal axis of the beam, it can be shown that the maximum vertical and horizontal deflections in a simply supported beam are

$$v_{\max} = \frac{M_{Tx} L^2}{8EI_{xx}} \quad (3-13)$$

$$u_{\max} = \frac{M_{Ty} L^2}{8EI_{yy}} \quad (3-14)$$

These maximum deflections occur at the mid-span of the simply supported beam.

3.2 Finite Element Analysis

To calculate the deflections and stresses resulting from the time varying temperature distribution in the Transrapid guideway, the finite element model (4) described in the previous section was used. The finite element program also calculated the thermal moments, deflections and stresses at each time step throughout the daily cycle. The results of this analysis are presented in the following section.

3.3 Numerical Results and Parametric Studies

The deflections in the vertical and horizontal directions and the bending stresses for the Transrapid Maglev guideway were calculated under a variety of conditions. These studies were

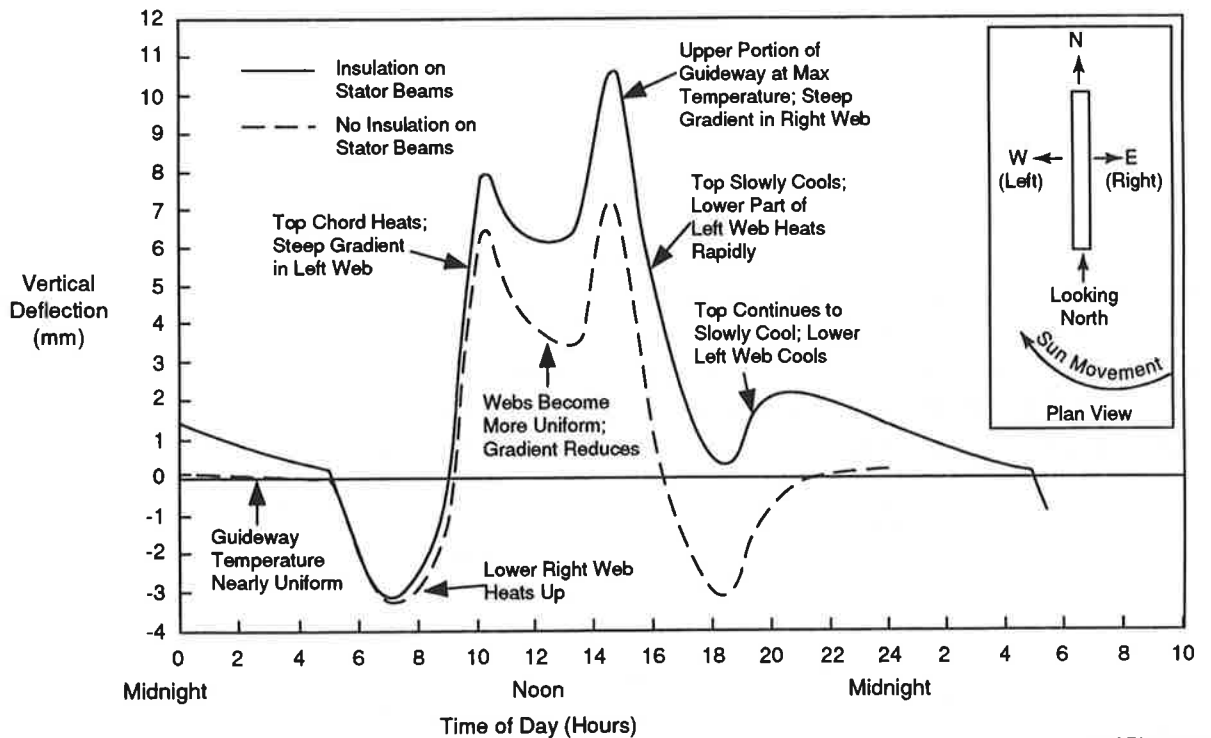
conducted to determine the worst case scenarios for deflection and stress. As discussed earlier in Section 2, the initial “baseline” case for thermal-structural studies was the early summer day (June 21 solstice, with highest sun angles), N-S orientation and plain steel surface. Later parametric studies across the range of combinations of guideway orientation and seasonal points did reveal slightly higher deflection maxima later (discussed in subsection 3.3.3 following), but the baseline is very useful for understanding the relationship between the daily heating and cooling of the guideway and the deflection and stress responses. The results are summarized below.

3.3.1 Vertical Deflection

The vertical deflections for a single span Transrapid guideway were initially calculated for the baseline summer day conditions (summer solstice, N-S orientation, plain steel surfaces) at 15 minute intervals throughout the day. The results are shown in Figure 3-2, which plots the midspan vertical deflection of the guideway for the “insulated” and “uninsulated” cases described earlier. As shown in the figure, the guideway deflection response throughout the day is quite complicated, due to the continually changing ambient conditions and position of the sun, and the complex geometry of the guideway. These effects are discussed below.

Nighttime/Early Morning Hours

Between the hours of approximately 10 pm and 6 am, the guideway temperatures are nearly uniform, resulting in very small vertical deflections. At sunrise, the lower portion of the right



218-DTS-9612-16

Figure 3-2. Vertical Deflection (Summer, 25m Single Span, N-S Orientation) versus Time of Day

web (East-facing web, when looking North) rapidly heats from direct sunlight, while the upper portion of this web is in the shade of the guideway side rail (these temperature effects were shown in Figure 2-11). The left web remains cool, as it is completely in the shade of the guideway. This rapid heating of the lower part of the right web causes a downward (negative) deflection, as shown in Figure 3-2.

Late Morning/Early Afternoon Hours

Later in the morning, as the sun rises higher in the sky, it begins to heat the top chord and the right side rail of the guideway. The lower portion of the right web begins to cool, and the upper portion of the both webs begins to heat up from the hot top chord. A significant vertical temperature gradient is formed in the left web, resulting in a deflection peak at approximately 11 am.

From approximately 11 am to 2 pm, the sun directly heats the top chord of the guideway, while both webs are in shade. (These temperature effects were also shown in Figure 2-11). The web temperatures start to become more uniform in the depthwise direction, reducing the vertical temperature gradient and deflection, as shown in the figures.

At approximately 2 pm, the sun begins to heat the left side rail and web of the guideway, while the lower portion of the right web cools. At this point, the rails and stator support beams are at their hottest temperatures of the day. These effects result in an even larger temperature gradient in the right web in the range of 30°C, and the maximum vertical deflection at the second peak, as shown in the figure.

Late Afternoon/Evening Hours

In the late afternoon, the top chord, rails and stator support beams begin to cool slowly, while the sun directly heats the lower portion of the left web. This rapidly reduces the temperature gradient, and results in decreasing vertical deflection. After the sun has set, the web temperatures again cool and become more uniform. However, the top chord, rails and stator support beams, which are relatively massive, have stored a large amount of heat during the day, and are cooling at a slower rate. These portions of the guideway are still warm compared to the webs, resulting in an increase of the upward deflection between the hours of 6 and 9 pm. Later in the evening, the upper part of the guideway finally cools, and the guideway is again essentially at a uniform temperature, with only a very slight vertical deflection.

From Figure 3-2, the largest deflections occur at 2:45 pm, with the "insulated" case having a maximum deflection of 10.7 mm for the single span. The deflections for the "uninsulated" case are smaller, with the maximum being 7.4 mm for the single span. The reduced deflection corresponds to the temperature gradient results presented in Section 2: the large surface area of the side rails and stator support beams readily allows heat to transfer out of the guideway, thereby reducing the thermal moment and the deflection in the uninsulated case.

For comparison purposes, the deflections induced by the fifth order New Zealand code temperature distribution were also calculated using the equations presented previously. For a single span 25m guideway, the New Zealand code results in vertical thermal deflections of 13.6 mm, which is somewhat greater than predicted by the FE model. (However, as noted previously, the New Zealand code cannot be used to evaluate horizontal deflections, since it ignores temperature variations in the horizontal direction.)

As noted in the previous sections, the "insulated" case corresponds to conditions in which the stator packs or other equipment are attached to the guideway, while the "uninsulated" case assumes the guideway does not have any equipment mounted on the stator support beams. The deflection results presented above thus indicate that the deflections for a guideway with equipment mounted on the stator support beams may be larger than the deflections in a guideway with no equipment attached.

3.3.2 Horizontal Deflections

The horizontal deflections for the baseline summer case, using the single span guideway, are shown in Figure 3-3. Both the "insulated" and "uninsulated" cases (with and without stator packs) have been calculated. The maximum horizontal deflection occurs in the late afternoon, when the sun is lower in the sky. As noted previously, under these conditions one web is in direct sunlight while the other is in shade. For the insulated case, the maximum deflection is

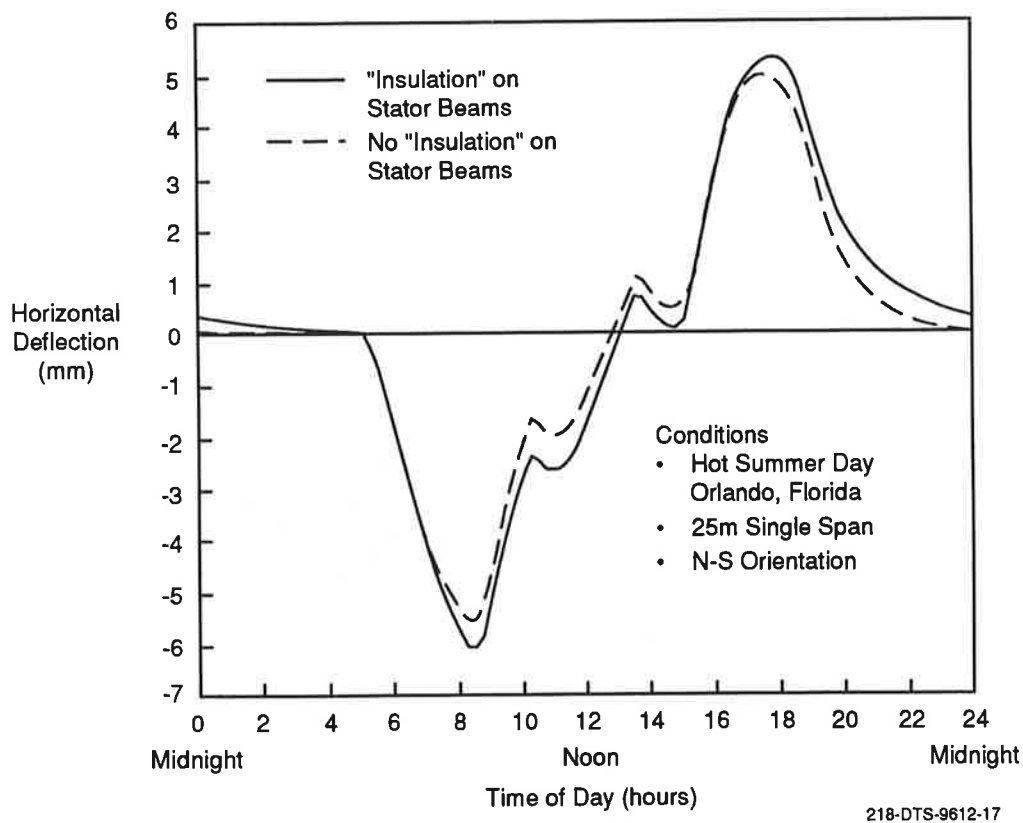


Figure 3-3. Horizontal Deflection versus Time of Day

approximately 6.0 mm. For the uninsulated case, the deflections are slightly smaller, with the maximum being approximately 5.5 mm. The reduced deflections are due to the effects of heat transfer near the side rails and stator support beams as described above.

3.3.3 Effects of Guideway Orientation and Season

Guideway Orientation

Initial studies using the summer baseline configuration were performed to determine the sensitivity of the vertical and horizontal deflections to the orientation (compass direction) of the guideway. The results are shown in Figure 3-4 using the simply supported, single span configuration. For this case, the maximum vertical and horizontal deflections both occur for the North-South guideway orientation. The minimum summertime deflections occur when the guideway is oriented in an East-West direction.

Seasonal Variations

A study similar to the above was performed under winter conditions, at the winter solstice (December 21) having minimum sun angles. For this study, average winter day conditions for Orlando were used, with ambient temperatures of $T_{max} = 22.8^{\circ}C$ ($73^{\circ}F$) and $T_{min} = 10.6^{\circ}C$ ($51^{\circ}F$). The results are shown in Figure 3-5, again for the simply supported single span

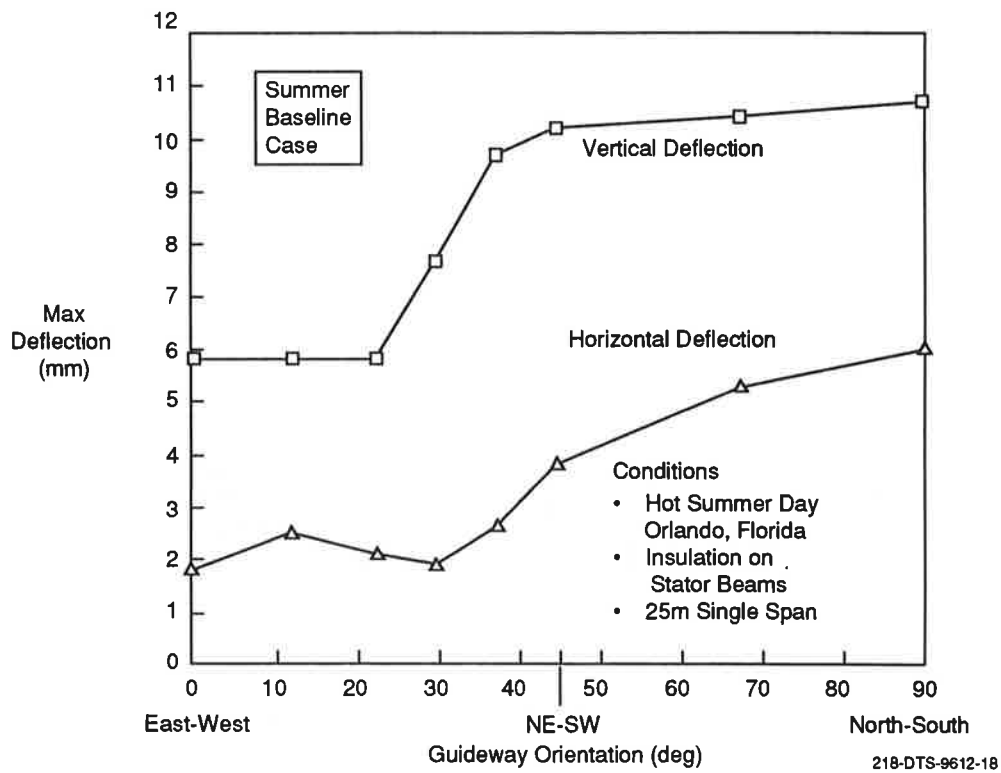


Figure 3-4. Effects of Guideway Orientation (Single Span), Baseline Case, Summer Conditions

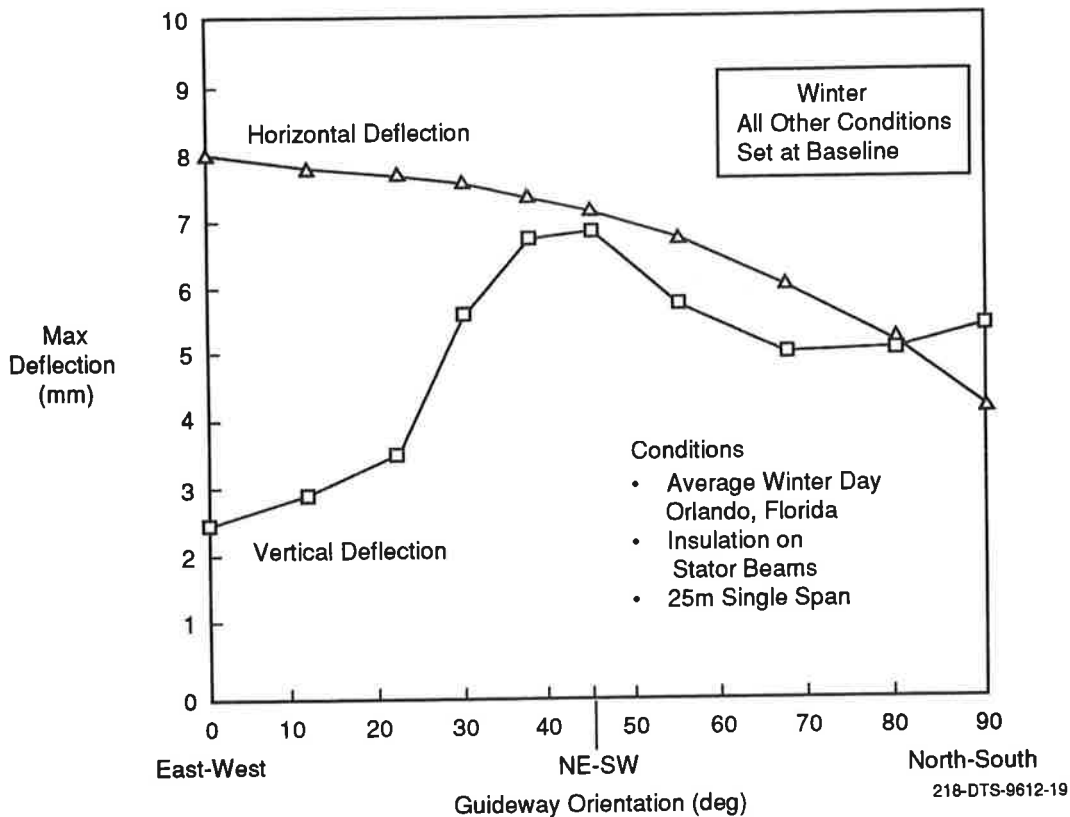


Figure 3-5. Effects of Guideway Orientation (Single Span)

configuration. The results indicate that during the winter season, the horizontal deflections can actually be larger than the vertical deflections for the majority of guideway orientations. This is due to the sun's position in winter, which is low on the horizon. This allows for long periods of direct solar heating of the guideway main webs, but prevents the efficient heating of the top chord of the guideway. The maximum horizontal deflection is approximately 8 mm, which occurs when the guideway is oriented in the East-West direction. As mentioned previously, such horizontal deflections (like the vertical deflections in summertime) could possibly exceed guideway operational tolerances or have safety implications for the Maglev system.

Combined Effects of Guideway Orientation and Season

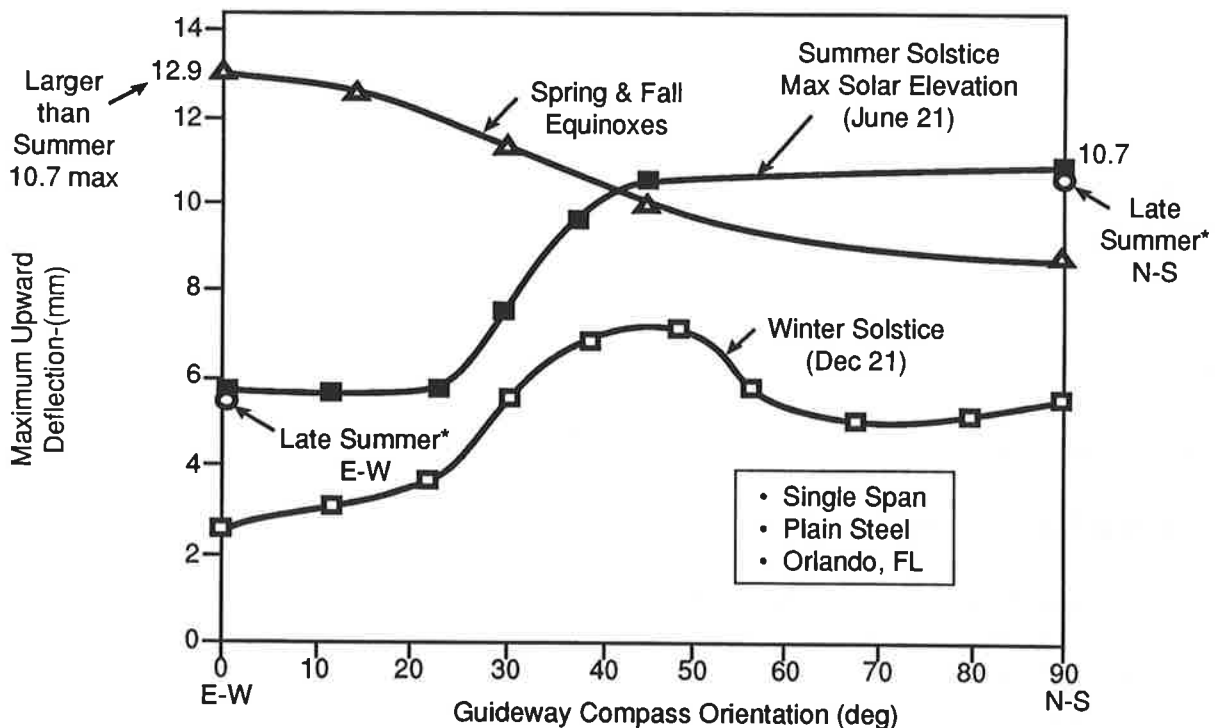
As discussed earlier in subsection 2.3.3, further studies with the heat transfer model indicated that the maximum daily transient thermal gradients, and hence deflections and stresses, were affected by the individual combination of orientation and season. Therefore, combinations of guideway orientations from N-S to E-W with different seasonal points were made. It was found that the E-W orientation in combination with the equinoxes produced a somewhat higher vertical deflection of 13 mm than did the baseline "summer solstice/N-S" case, and that the E-W direction in combination with the mid-winter point did produce the highest horizontal deflection of 8 mm. The full orientation range was explored for the equinoxes (March 21 and Sept. 21), and the halfway points between summer solstice and equinox were also checked for N-S and

E-W (these latter deflections were very close to those for the solstice). The thermal properties of the plain steel surfaces, and the simply supported single span condition were used, as before.

Figure 3-6 summarizes the complete vertical deflection picture for the full range of combinations of guideway orientation and season. It can be seen how the vertical deflections will likely remain below a “bound” of approximately 11 mm (N-S) to 13 mm (E-W) for all seasons, but that the deflections are likely smaller in the six “winter” months between the fall and spring equinoxes. This plot could also be used in route alignment planning to predict the most likely zones of large guideway deflections.

A similar summary plot for the horizontal deflections is shown in Figure 3-7. Here, it can be seen that the additional combinations of season and orientation did not produce deflections larger than the initial cases discussed above in subsection 3.3.2; the largest horizontal deflection of 8 mm remained the winter December 21/E-W case. The upper bound in this case seems to be the 8 mm/E-W to 6 mm/N-S line.

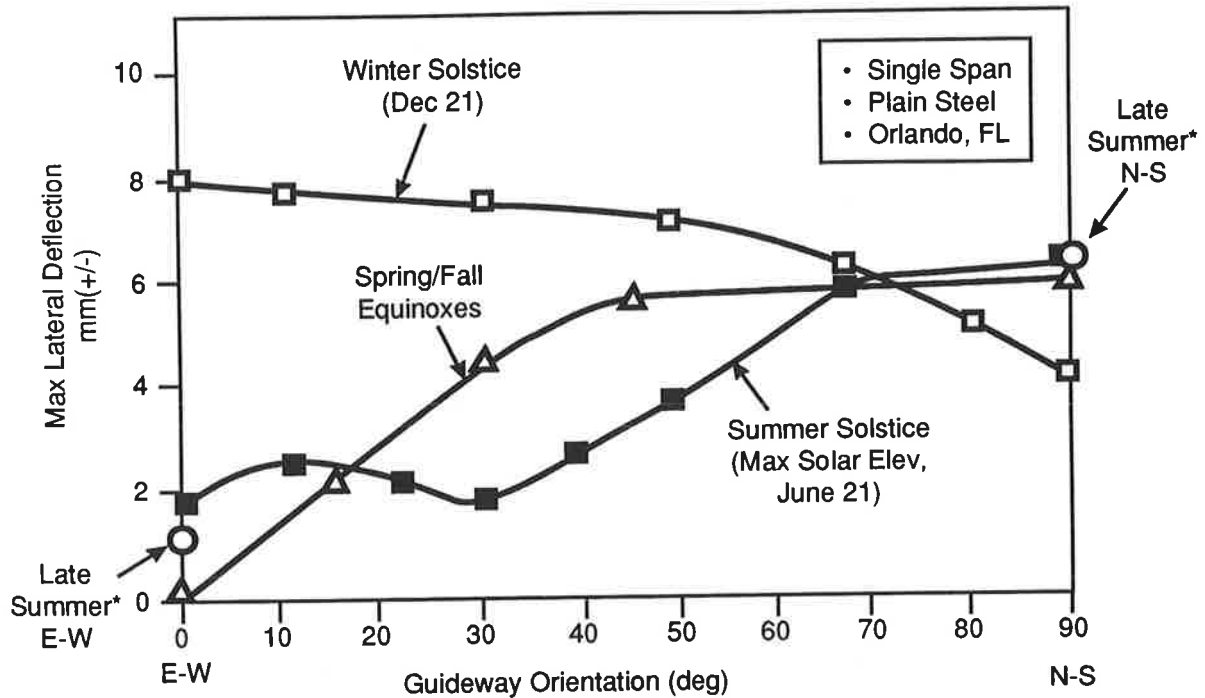
The deflections in both these cases being in the range of 8 to 13 mm are significant in comparison to the 8 mm gap, and indicate that both the vertical and horizontal deflections should be considered for the testing and service use of the guideway in Florida.



*Late Summer=Midway between Solstice & Equinox (~Aug.6)

217-DTS-9612-3

Figure 3-6. Maximum Vertical Deflection versus Orientation and Time of Year



*Late Summer=Midway Between Solstice & Equinox (~Aug. 6)

217-DTS-9612-1

Figure 3-7. Maximum Horizontal Deflection versus Orientation and Time of Year

3.3.4 Effects of Surface Treatments on the Guideway

As noted previously, the surface treatment of the guideway can significantly influence the guideway temperatures and thermal deflections. Parametric studies were conducted with the finite element model to determine the effects of the guideway surface treatment on the vertical and horizontal deflections. The effects of oxidation (rust) and white paint on the top surface of the guideway were examined for summer and winter conditions, with guideway orientations of 90 deg (North-South) and 0 deg (East-West), and the results were compared to the baseline case of untreated steel. The results of this study are presented in Table 3-1 for a simply-supported guideway beam. The results indicate that there is only a slight difference in deflection between the untreated steel guideway and the oxidized steel guideway, each of which has a maximum vertical deflection in the range of 10 to 11 mm, occurring in summer when the guideway is oriented in the North-South direction. Similarly, both the untreated and oxidized steel guideways have a maximum horizontal deflection in the range of 7 to 8 mm, occurring in winter when the guideway is oriented in the East-West direction. For the guideway with the super-white top coating, however, the deflections are significantly reduced. The maximum “baseline case” vertical deflection for the guideway with super-white paint is only 2.0 mm (summer, N-S orientation). This represents a reduction of approximately 80 percent in comparison to the baseline, plain steel case. Similarly, the maximum horizontal deflection for the guideway with super-white paint is only 1.4 mm, which occurs in winter when the guideway is oriented in the

Table 3-1. Effects of Guideway Surface Treatment of Thermal Deflection

Surface Treatment	Season	Orientation	Maximum Deflections (mm)	
			Vertical	Horizontal
Untreated (plain) $\alpha_s = 0.6$ $\epsilon = 0.2$ $\alpha_s/\epsilon = 3$	Summer	N-S	10.7	6.0
	Summer	E-W	5.8	1.9
	Winter	N-S	5.5	4.4
	Winter	E-W	2.4	8.0
Oxidized Steel $\alpha_s = 0.8$ $\epsilon = 0.8$ $\alpha_s/\epsilon = 1$	Summer	N-S	10.4	6.1
	Summer	E-W	5.7	2.0
	Winter	N-S	6.0	4.7
	Winter	E-W	1.9	7.5
"Super-White" Paint $\alpha_s = 0.15$ $\epsilon = 0.9$ $\alpha_s/\epsilon = 0.2$	Summer	N-S	2.0	1.1
	Summer	E-W	1.1	0.4
	Winter	N-S	1.0	0.9
	Winter	E-W	0.8	1.4
Notes: 25m single spans Insulation on stator support beams				

East-West direction. Again, this represents a reduction of approximately 80 percent compared to the baseline case. These results thus indicate that coating all surfaces of the guideway with white paint can be a very effective means of reducing the guideway thermal deflections. The issue then will be if such a coating can be maintained in actual service, retaining the high reflectivity required in order to be effective.

The "super-white" coating discussed above represents the most highly reflective coating achievable in a laboratory-type situation, and is useful to estimate the biggest gradient and deflection reductions attainable. However, a more realistic set of coating properties representing the in-service white-painted guideway would clearly provide less of a reduction. For this reason, a range of vertical deflections for the baseline configuration representing these situations was calculated, as discussed earlier in subsection 2.3.4. (Recall this described the thermal surface properties for the range of new and deteriorated white coatings.) This is summarized in Figure 3-8, which estimates the practical degree of reduction in vertical deflections that might be relied upon in service. A range of 30 to 60 percent is suggested, depending on the exact paint composition, application technique, and, most important, deterioration. These estimates used available thermal properties of selected commercial paints as guidelines (15).

Since the reductions can be substantial, the actual coating performance over time should be carefully evaluated by field tests or other accepted accelerated aging tests as part of the final design, to establish a safe margin of performance that can be assured in service.

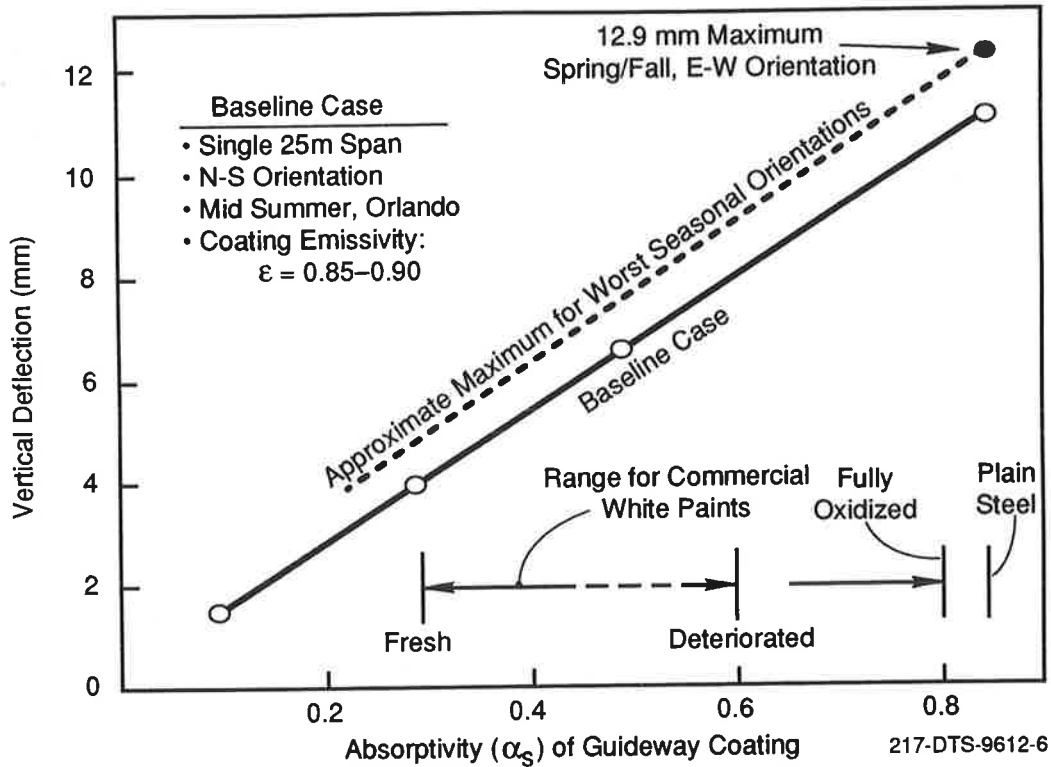


Figure 3-8. Effectiveness of Guideway Coatings in Reducing Thermal Deflections

3.3.5 Effects of Ground Radiation and Convection

As noted previously in subsection 2.3.5, the guideway may also be subject to additional heating from ground radiation (both direct and reflected) and convection. Parametric studies were conducted to determine the effects of this additional heating on the guideway deflections. The thermal deflections were calculated for several guideway heights above ground level. The results of this study are shown in Figure 3-9, which presents the maximum upward and downward deflections of the guideway for two ground conditions: a typical concrete ground surface (reflectivity = 0.5), and a more highly reflective ground surface (reflectivity = 0.85) which allows a greater amount of reflected solar radiation to reach the lower portion of the guideway. The results show that for both ground conditions the upward deflections are slightly reduced when the guideway is mounted close to ground level due to the ground radiation/convection heating of the bottom chord. This heating effect also tends to increase the maximum downward deflection of the guideway. As the guideway height above ground level increases, the ground heating influence on the deflections is reduced. At a guideway height of approximately 5m above ground level, the ground heating effects are quite small, and the guideway deflections are essentially unchanged from the baseline case, in which ground radiation and convection effects were not considered. The analysis also has shown that the horizontal deflections, although not shown here, were essentially unaffected by ground radiation and convection.

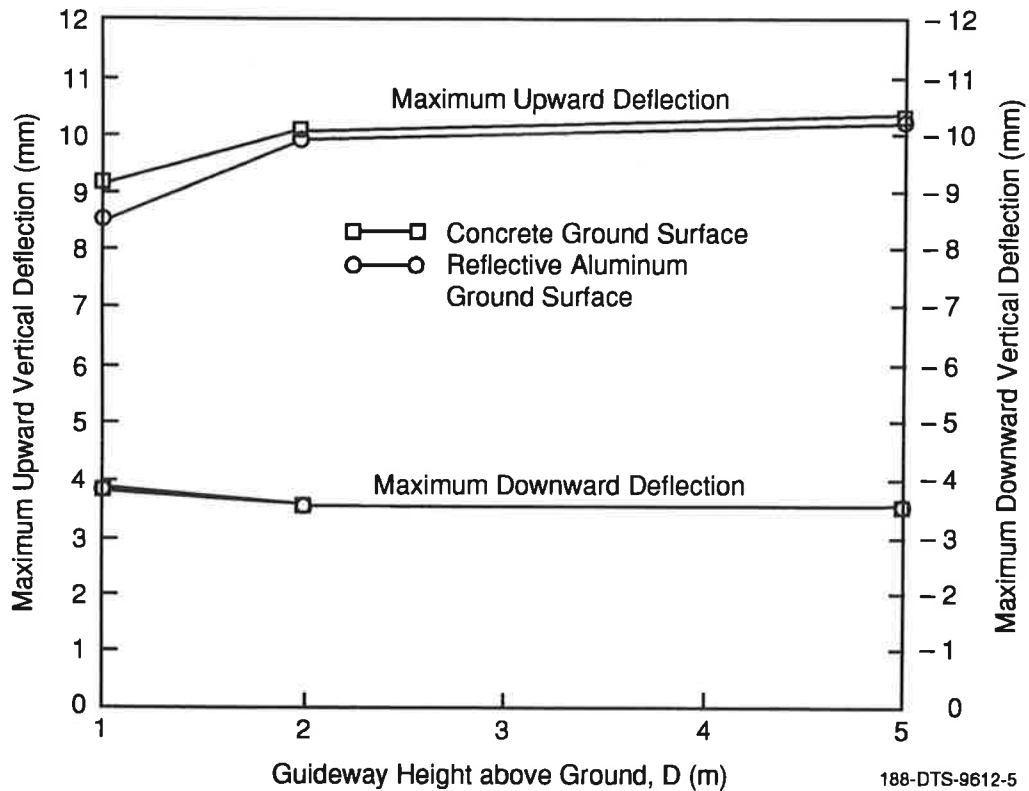


Figure 3-9. Effects of Ground Radiation/Convection on Vertical Deflections

It must be noted here that these results are approximate, since in the finite element model the ground radiation and convection effects were considered to affect only the bottom chord of the guideway. However, this analysis does indicate that while ground radiation and convection may influence the maximum guideway vertical deflections, both upward and downward, the effects may be expected to be minor.

3.3.6 Effects of Vehicle Induced Heating

As noted in previous sections, the passage of the Maglev vehicle dissipates power in the stator packs, which results in heating of the windings and iron in the stator pack. Quantification of the changes in guideway deflection caused by vehicle induced heating cannot be accurately determined from the amount of information currently available on the stator pack design, and details of the stator pack attachment to the guideway. However, due to the location of the stator packs, these heating effects are expected to increase the temperatures in the upper portion of the guideway, particularly in the region of the stator support beams, the upper portion of the webs, the top chord, and the side rails. Since these parts of the guideway structure all lie above the centroid of the cross section, the heating effects increase the thermal bending moment about the horizontal axis, resulting in increased upward vertical deflections. The heating effects may be significant, especially in cases of a series of vehicles traveling at relatively low speed, such as near a station. The heating effects may be particularly severe when the additional effects of levitation and guidance losses are considered (due to insufficient data, only propulsion power

losses and heat generation have been considered here). The cyclic thermal loads generated by the vehicle may be significant, and may also affect the bolt attachment of the stator packs to the guideway. There currently is insufficient data available to quantify these effects. These effects warrant further investigation and testing to determine the amount of heating induced in the guideway, the resulting increase in thermal deflection and stress, and the possible effects on the stator pack attachment bolts.

3.3.7 Double Spans versus Single Spans

The deflection and stress results presented above are representative of the Transrapid steel Maglev guideway using a 25m single span. However, the proposed Florida system may also use double span guideways with a continuous support at the center pylon (see Figure 3-10). The results obtained for the preceding analysis for single span can be readily translated to double span guideways, as shown below.

It is assumed here that the center support design restrains both the vertical and horizontal deflections at the center support to zero. Then for a double span guideway which has a total beam length of $2L$ (as shown in Figure 3-10), it can be shown that the maximum vertical and horizontal deflections due to the combined effects of the thermal moments and the restraint at the center support are given by

$$v_{\max, \text{double}} = \frac{M_{Tx} L^2}{27EI_{xx}} \quad (3-15)$$

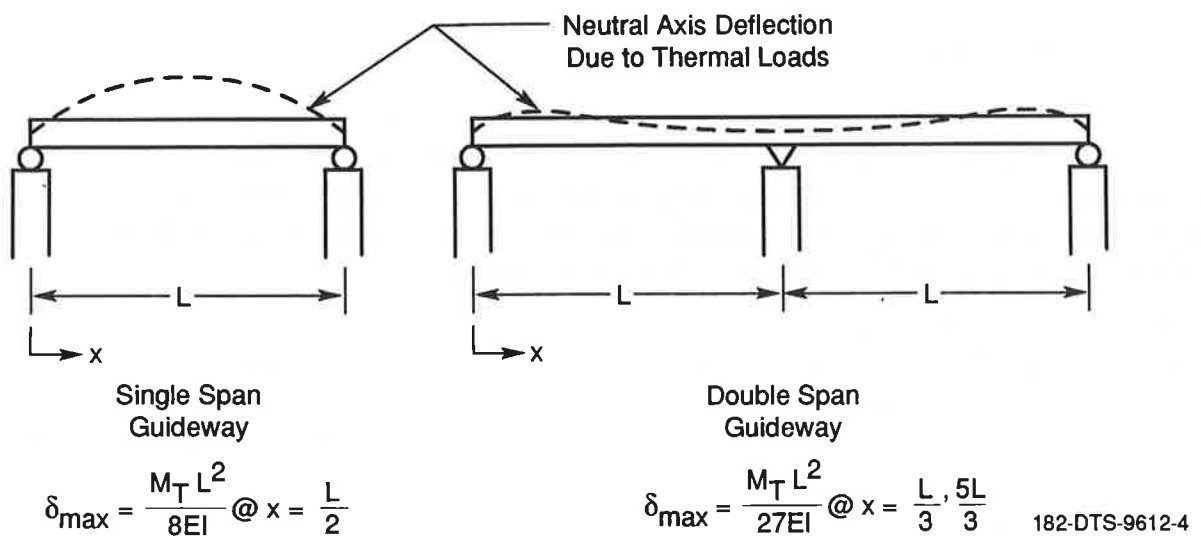


Figure 3-10. Thermal Deflection in Single and Double Span Guideways

$$u_{\max, \text{double}} = \frac{M_{Ty} L^2}{27EI_{yy}} \quad (3-16)$$

Referring back to equations (3-13) and (3-14), this implies that

$$\left(\frac{v_{\max, \text{double}}}{v_{\max, \text{single}}} \right) = \left(\frac{u_{\max, \text{double}}}{u_{\max, \text{single}}} \right) = \frac{8}{27} \approx 0.3 \quad (3-17)$$

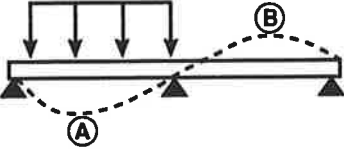
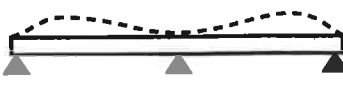
In other words, the maximum thermal deflections in a double span guideway are approximately 30 percent of the thermal deflections in a single span guideway, all other conditions being equal. Thus, all of the preceding deflection results for the 25m single span guideway (including the parametric studies of guideway orientation and seasonal variation) can be applied to a double span guideway (total beam length of 50m) by multiplying by the factor of 8/27. This implies that the maximum vertical deflections for a double span guideway are approximately 4 mm* (This assumes plain steel surfaces) while the maximum horizontal deflections are approximately 2.4 m (winter).

A useful comparison can be made of the thermal versus static live load vertical deflections for the double span configuration. This puts the thermal deflections in perspective with other contributions to overall guideway response. For the double span beam, also known as “alternating continuous” configuration, the highest downward live load (static vehicle weight) deflections are produced when one of the two spans is loaded. The unloaded span deflects upward about half the amount of the downward span. Figure 3-11 shows this effect, together with a summary of vertical deflections for both spans. (Note that we are using static vehicle weights for this comparison, not amplified by any dynamic effects from vehicle-guideway interaction.) The 4 mm thermal deflections are of the same order as those for the static live load, and it can be seen that the total of the static live load and thermal deflections then produces a range of ± 7 mm of vertical response for the double span.

Another important issue with regard to the deflections of single and double span guideways is the discontinuity of slope that occurs at the beam ends. Figure 3-12 schematically shows the discontinuity of slope between two adjacent guideway beams at a support pylon. This sudden change in the slope of the guideway may affect the vehicle ride quality. For a single span guideway, the vertical slope at either end of the guideway beam is given by

$$\theta_{\text{single}} = \pm \frac{M_{Tx} L}{2EI_{xx}} \quad (3-18)$$

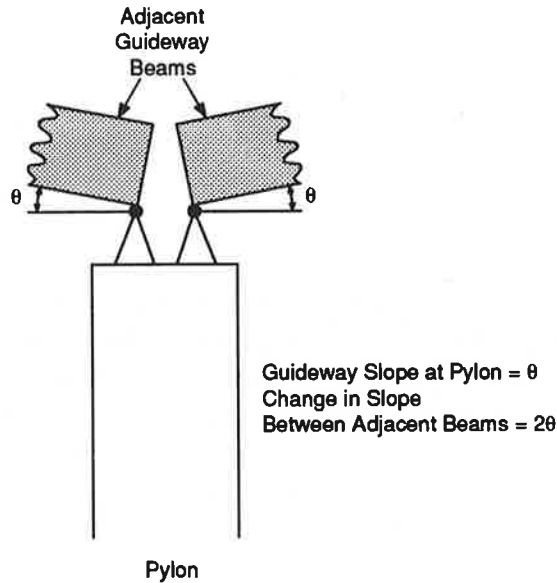
* $\frac{8}{27} \times 13 \text{ mm}$

			
	Vehicle Loading*	Thermal Loading	Total
Max Downward Deflection (-)	- 6 mm at A	- 1 mm	- 7 mm
Max Upward Deflection (+)	+ 3 mm at B	+ 4 mm	+ 7 mm

* Static Vehicle Weight of 19.6 kN/m Applied to One Span of Double-Span Beam

217-DTS-9612-7

Figure 3-11. Deflection Comparison of Thermal and Static Live Loads for Double Span Guideway Configuration



187-DTS-9612-3

Figure 3-12. Slope Discontinuity Between Adjacent Guideway Beams

$$\sigma_{CR} = \frac{k\pi^2 D}{tb^2} \quad (3-20)$$

where:

σ_{CR} = critical plate buckling stress

t = top chord plate thickness (16 mm)

b = plate width between support webs (1.96m)

a = unsupported panel length; max = b w/no diaphragms

$D = \frac{Et^3}{12(1-\nu^2)}$ flexural rigidity

E = 206.85 GPa (steel)

k = numerical factor based on plate length and width = $\left(\frac{a}{b} + \frac{b}{a}\right)^2$

ν = Poisson's ratio = 0.3

For the case described above, k = 6.1, and the critical buckling stress is

$\sigma_{CR} = 76 \text{ MPa (11 ksi)}$

Note that if the diaphragm stiffeners are not present, or if they offer insufficient resistance to buckling of the top chord, then the buckling half-wavelength will approximate the width, and the numerical factor, k, is 4.0 (11). The critical buckling stress for this case is then reduced to

$\sigma_{CR} = 50 \text{ MPa (7.2 ksi)}$, or 1/3 lower than with diaphragms at 1.0m.

The calculated compressive stresses on the guideway top chord due to the thermal, dead and live loads are listed in Table 3-2 for the single and double span cases (untreated steel). Note that the thermal compressive stresses for the single span range from 27.6 to 34.5 MPa (4 to 5 ksi), but increase up to 39.3 to 57.9 MPa (5.7 to 8.4 ksi) for the double span case, due to the restraint at the center pylon support. The stress increments due to the dead and live loads (shown in the table) further increase the top chord compressive stresses at the mid span for both the single span and double span cases (note that the compressive stresses at the center pylon in the double span case are actually reduced by the dead and live loads). The sum of the thermal, dead and live loads yields a maximum top chord compressive stress of 50.1 to 57.0 MPa (7.3 to 8.3 ksi) in the

Table 3-2. Summary of Stresses in Guideway Top Chord

Load	Max Top Chord Compressive Stress		
	Single Span at Midspan	Double Span	
		Midspan	At Center Pylon
Thermal	27.6 to 34.5 MPa (4 to 5 ksi)	39.3 to 46.2 MPa (5.7 to 6.7 ksi)	51.0 to 57.9 MPa (7.4 to 8.4 ksi)
Dead Load*	8.3 MPa (1.2 ksi)	4.8 MPa (0.7 ksi)	-20.7 MPa (Tension) (-3.0 ksi)
Live Load**	14.2 MPa (2.1 ksi)	11.0 MPa (1.6 ksi)	-6.9 MPa (Tension) (-1.0 ksi)
Total: Thermal + Dead + Live Loads	50 to 57 MPa (7.3 to 8.3 ksi)	55 to 62 MPa (8.0 to 9.0 ksi)	23 to 30 MPa (3.4 to 4.4 ksi)
<p>Notes:</p> <p>Thermal stress range is for seasonal/orientation band of maxima.</p> <p>*Dead load assumes a guideway weight of 10.66 kN/m (61 lb/in.) plus guideway equipment of 1.07 kN/m (6 lb/in.).</p> <p>**Live load assumes a static vehicle weight of 19.6 kN/m (112 lb/in.) even distributed over the single span, or over one span of the double span guideway, to yield maximum bending stress.</p>			

single span, and 55.1 to 62.0 MPa (8.0 to 9.0 ksi) in the double span. Note that these stress levels could increase somewhat, since the assessment of live load did not consider any dynamic interaction effects between the vehicle and guideway, which can increase the live load deflections and stresses.

The calculated stress results listed above are approaching the local buckling strength (75.8 MPa, 11.0 ksi) predicted for the top chord, and exceed the buckling strength of the case in which the diaphragms are not present or are ineffective (49.8 MPa, 7.2 ksi). In view of the additional dynamic interaction effects on the live load, there may be insufficient margin for local buckling safety on the top chord of this guideway. To provide greater margin of safety, the buckling strength of the top chord could be increased by increasing its thickness, or by using a closer diaphragm spacing with sufficiently rigid diaphragms. Another approach could use a longitudinal web stiffener down the centerline of the top chord. Use of white coating on the guideway would also greatly reduce the thermal stress component. However, each of these methods requires further study or tests to determine if the local buckling potential can be successfully eliminated.

The results of this analysis thus indicate that the thermal stresses, and local buckling of the top chord, should be considered in the design and implementation of any guideway system chosen for use in the Florida environment.

3.3.9 Thermal Fatigue

Fatigue concerns are present in any transportation support structure, including welded steel guideway beams. The thermal stresses potentially could contribute in two ways: as direct cyclic stresses, and as a mean-stress raiser for the primary cyclic stresses, which are the live vehicle loads. The direct cyclic contribution will likely be small over a 20-year life since a cyclic accumulation in the range of only 5000 cycles or so would be possible with daily cycling at the max stress for a majority of the days per year. This is in the low cycle fatigue (LCF) regime, and cyclic stresses large enough to cause problems in this region must be avoided, and presumably have been in this design. However, the effective mean stresses could be raised significantly when thermal stresses occur, and these should be checked in detail. Not only the potential fatigue effects on both overall beam bending, but, more importantly, local transverse bending of the top chord should be evaluated.

A preliminary estimate of these effects can be made using generic data. Fatigue data for the family of A36-A441-A514 steels, in welded construction (16) is shown in Figure 3-14. This particular data also shows little variation with mean stress level for mean stresses in the range of -6 to +10 ksi (meaning the primary effect is due to stress range, or alternating stress double amplitude). If this is true for the steels and manufacturing process used in the Transrapid guideway, then the addition of mean thermal stresses to dead loads and built-in stresses already present might also have little effect.

To gauge the scope of the stresses that might be involved, we can use the above generic welded steel fatigue data at a typical location on the cross-section. (For example, the minus-2 sigma stress range for 10^6 cycles is about 10 ksi, which could be compared against the cyclic live load stresses.) For transverse bending of the upper chord plate at the point of web support, and

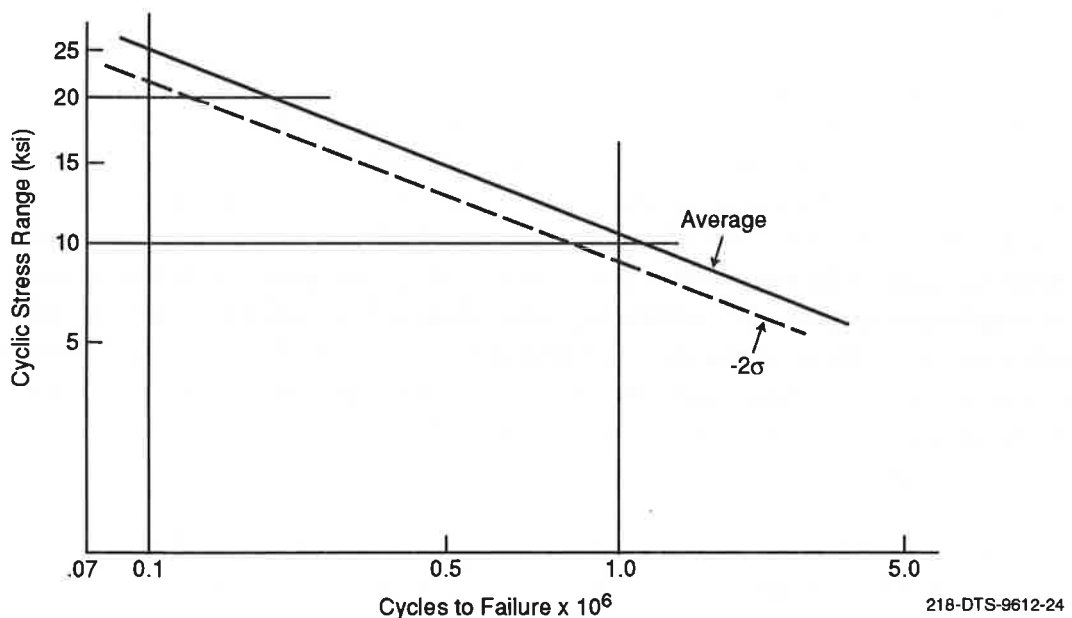


Figure 3-14. Generic Fatigue Data for A-36 Steel in Welded Construction (16)

using the live and dead loads cited in Table 3-2, dead load effects might be 3 ksi, and live load effects (cyclic stress range with a possible dynamic load factor of 2.0) could be 16 ksi. Adding the transverse effects of 6 to 8 ksi thermal compression in the perpendicular (longitudinal) direction to the dead load stresses, the mean stress might increase from 3 to 6 or 7 ksi. (Transverse bending stresses due to local thermal buckling tendency would be additional.) If this increased total mean stress does not lead to higher cyclic damage from the live load stresses for the exact TR material and process, then the fatigue life would be close to that without the thermal component. The adequacy of this fatigue life itself is a separate subject not addressed here.

These aspects should be evaluated using the approach of (16,17), or their equivalents. These TRB publications are respectively entitled, "Effects of Weldments on Fatigue Strength of Welded Steel Beams," and "Fatigue of Welded Steel Bridge Members Under Variable-Amplitude Loadings."

3.4 Summary of Deflection/Stress Analysis

The results for the finite element deflection and stress analysis of the Transrapid Maglev guideway beam are summarized below:

- For the 25m single span, plain steel guideway in the Orlando environment, vertical deflections up to approximately 13 mm can occur in the operational guideway with equipment mounted on the stator support beams. The deflections are smaller (approximately 9 mm) for the beam without any equipment.
- Horizontal deflections of the guideway can reach 8 mm for single spans due to the solar heating of one main web during morning or late afternoon hours.
- The FE model predicts vertical deflections which are slightly lower than those calculated using the New Zealand design code. However, none of the design codes (including the New Zealand code) account for the horizontal deflections predicted by the detailed analysis presented here.
- Parametric studies using the FE model have shown that guideway orientation and seasonal effects can influence the guideway deflections. Vertical deflection cases evaluated to date are bounded by a 13 mm maximum for the E-W orientation (Mar 21/ Sep 21 equinoxes) and 11 mm for the N-S orientation in a 3+ month period centered on June 21 (summer solstice). Maximum horizontal deflections up to 8 mm occur in winter, with the guideway oriented more in the East-West direction.
- A white coating on the guideway can significantly reduce the thermal deflection in comparison to the untreated steel or oxidized steel guideways. Practical coatings in service can reduce deflections by 30 to 60 percent, with even higher reductions using "laboratory" coatings. Tests will be required to determine proper in-service coating performance.

- Use of a double span guideway configuration reduces deflections by 70 percent in comparison to single spans, due to the beam continuity over the center pylon support. A comparison of single and double span maximum deflections for plain steel guideway is shown in Table 3-3.
- Radiation and convection from the ground can heat the lower portion of the guideway, resulting in a small reduction of the vertical deflection. The effect is greatest when the guideway is mounted close to the ground on short pylons.
- Ambient air temperatures do not influence deflections nearly as much as the geometric sun angle factors or other conditions such as support configuration or guideway coating. High climatic temperatures are not required to produce the largest deflections and stresses.
- Thermal stresses in the top chord are typically in the range of 28 to 35 MPa (4 to 5 ksi) for single span, and 39 to 58 MPa (5.7 to 8.4 ksi) for double spans, using plain steel guideway surfaces. These stresses, when combined with typical dead and live load stresses, may approach the critical local buckling strength of the top chord. White coatings will reduce the thermal stresses, and structural modifications can raise the buckling strength.
- Vehicle induced heating of the stator packs can increase temperatures in the upper portion of the guideway, resulting in increased vertical deflections. Quantifying these effects requires further study and testing, and must include effects of slow, stopped and/or frequent vehicles.

**Table 3-3. Maximum Thermal Deflection Summary
(Plain Steel Guideway)**

	Single 25m Span	Double Span (2 x 25m)
Vertical	13 mm	4 mm
Horizontal	8 mm	2.5 mm

4. SAFETY IMPLICATIONS FOR THE TRANSPRAPHIC MAGLEV GUIDEWAY

This study is part of the overall effort to identify and evaluate safety related aspects of Maglev system performance. For the Orlando location, the magnitudes of the thermally-induced deflections and stresses clearly can span a wide range depending on the specific configuration used. The peak deflections seen for the plain steel, simple span beam, for example (13 mm vertical upward, and 8 mm laterally), would in all likelihood, present significant safety problems for the system, not to mention effects on ride quality and guideway life. However, mitigation via use of a double span configuration in conjunction with white coatings could reduce these by a factor of four or possibly more, moving them to a status of one of many contributors to the total deflections.

4.1 Thermal Deflections

It is important to note that thermal deflections are only one of several contributors to the overall deflection "budget" which would be calculated for the full envelope of guideway conditions in service. These include not only the thermal and static live load deflections mentioned earlier in this report, but also the several contributions of guideway beam manufacturing accuracy, installation accuracy, pylon settlements, long-term creep or relaxation of guideway components, and dynamic effects of vehicle passage. These can vary in magnitude, direction and location on the guideway, and so this budgeting is a complex process when all effects are properly considered. This information was not available to Foster-Miller.

Nevertheless, some overall assessment of the significance of these thermal deflections might be made here, by comparing the deflections both with the nominal running gaps between vehicle and guideway for the Transrapid system, and with the predicted static live load deflections. (This latter was done for the plain steel, double span configuration in subsection 3.3.7)

Taking the case of vertical thermal deflections, Table 4-1 shows these comparisons together with the estimated significance these may have for safety. As can be seen, this implies that single spans should be avoided in the network unless special system considerations allow their use in selected locations (e.g., short spans, covered or shaded sections, slow speed areas, redesigned cross-sections, etc.). Further, the white coating seems to be effective in promoting the goals of safe operation, and this warrants lab and field testing to assure performance.

Similar conclusions can likely be reached in the case of the horizontal deflections.

5.2 Thermal Deflections and Stresses

- For the 25m single span guideway in the Orlando environment, vertical deflections of up to 13 mm can occur. This is for a plain steel guideway with stator packs installed. A bare guideway structure has approximately a 30 percent smaller response.
- Maximum vertical deflections can exceed 11 mm over the majority of the year for the same plain steel, single span guideway.
- Horizontal (transverse) deflections can reach 8 mm for a simply supported, plain steel single span, due to solar heating of one main web during early morning or late afternoon hours. Since the design codes do not account for horizontal variations in the temperature distribution, they cannot be used to estimate horizontal deflections of the guideway.
- Parametric studies have shown that the guideway orientation and seasonal effects in combination significantly influence the guideway deflections. The vertical deflections of 11 mm occur in the summer period with the guideway oriented more in the North-South direction, while the highest maximum of 13 mm is reached in the spring and fall for an E-W orientation. Maximum horizontal deflections occur in winter, when the guideway is oriented in the East-West direction. During winter, the horizontal deflections can be larger than the vertical deflections.
- The temperature gradients and deflections are strongly dependent on the surface treatment of the guideway. The deflections for untreated (plain) steel or oxidized steel guideways are approximately equal. However, a white coating on all surfaces of the guideway can significantly reduce the temperatures, deflections and stresses. A reduction of 30 to 60 percent for practical coatings in service may be achievable but must be verified by tests, including effects of deterioration.
- Use of a double span guideway configuration significantly reduces deflections in comparison to single spans. The maximum predicted deflections for a double span guideway (2 spans of 25m continuous over a center support) are approximately 4 mm in the vertical direction, and 2.5 mm in the horizontal direction.
- The maximum thermal stresses for the guideway, when combined with the vehicle loads, indicate a potential for local buckling of the guideway top chord, particularly for the double span guideway, which has higher stresses. A white coating can significantly reduce the stresses, and buckling strength can also be increased by design modifications. The results indicate that the potential for local thermal buckling of the guideway should be considered in the guideway design.
- Ground radiation and convection to the underside of the guideway may reduce guideway upward deflection, and increase its downward deflection. These effects are small unless the guideway is mounted close to ground level.

- Preliminary analysis of the vehicle-induced heating effects has shown that the guideway stator pack windings may heat up significantly due to vehicle passage, especially if the vehicle is stationary or if a series of many vehicles are traveling at short headways. These effects may be expected to increase guideway temperatures and deflections, but further study is required to be conclusive.

5.3 Recommendations

- The magnitude of the vertical *and* horizontal deflections due to thermal effects indicates that these should be considered in the operational safety and ride quality assessment of the guideway. Since existing design codes may be of limited use, an analytical approach incorporating finite element transient thermal analysis should be used. This must also include the capability of properly accounting for all geometric sun angle effects throughout the 24 hr day at any time of the year.
- The theoretical results presented here must be verified by an experimental program, prior to the final formulation of the conclusions on the safety of the Maglev guideway.
- The effects of white coatings on reducing the thermal response should be evaluated including the effects of aging and deterioration in service.
- Consideration should be given to experimentally validating the effects of equipment mounted on the guideway, and the effects of vehicle-induced guideway heating, both of which are expected to increase the thermal deflections of the guideway.
- The potential for local thermal buckling of the guideway should be investigated during the guideway design process. The analysis has shown that the thermal compressive stresses on the top chord may increase the potential for local buckling under combined thermal and vehicle loads, particularly for double spans.

6. REFERENCES

1. "Temperature Measurement on the TVE Steel Guideway Beam," Thyssen Henschel Technical Report, No. NVA/2647/09/88, September, 1988.
2. Personal communication with Dr. Mohsen Shahawy, Director of Research Programs, Florida Department of Transportation.
3. Samavedam, G. and Purple, A., "Thermal Effects and Mitigation Methods for Continuous Sheet Guideways," DOT Report No. FRA/NMI-92/1, Final Report, March 1992.
4. Elbadry, M. and Ghali, A., "User's Manual and Computer Program FETAB," University of Calgary, Canada, 1982.
5. Holman, J.P., *Heat Transfer*, 5th edition, McGraw-Hill Book Company, New York, 1981.
6. Bolz, R. and Tuve, G. (editors), *CRC Handbook of Applied Engineering Science*, 2nd edition, CRC Publishing, 1976.
7. "Annual Summary of Local Climatological Data, 1990," excerpt obtained from the National Oceanic and Atmospheric Administration, Library and Information Services Division, Rockville, MD.
8. Hoffman, P., McClure, R., and West, H., "Temperature Study of an Experimental Segmental Concrete Bridge," *Prestressed Concrete International Journal*, March-April 1983.
9. Heinrich, K., and Kretzschmar, R. (Editors), "Transrapid Maglev System," published by Transrapid International and Hestra-Verlag.
10. Boley, B., and Weiner, J., *Theory of Thermal Stresses*, John Wiley and Sons, New York, 1960.
11. Timoshenko, S. and Gere, J., *Theory of Elastic Stability*, Second Ed., McGraw-Hill, New York, 1961.
12. Campbell, T.I., and Siu, S.W., "Thermal Deformations in Typical Maglev Guideway Structures," *Journal of Advanced Transportation*, Vol. 21, pp. 215-226, winter, 1988.
13. "Thermal Analysis of Transrapid Guideway Proposed for Elevated Structures in Las Vegas-Southern California Corridor," report prepared the Canadian Institute of Guided Ground Transport (CIGGT), Report No. 86-13, September 1985.
14. Chapman, S.J., *Electric Machinery Fundamentals*, Second Ed., McGraw-Hill, New York, 1991.
15. Touloukian, Y.S. & DeWitt, D.P., *Thermal-Physical Properties of Matter*, Vol. 9, Coatings, CINDAS/Purdue University, pub. by Defense Logistics Agency DTIC-AI, Contract F33615-68-E1239, 1970.
16. Fisher, J., Frank, K., et al, "Effect of Weldments on the Fatigue Strength of Steel Beams," NCHRP Report No. 102, Highway Research Board, 1970.

17. Schilling, K., Klippstein, K., et al., "Fatigue of Welded Steel Bridge Member Under Variable-Amplitude Loadings," NCHRP Report No. 188, Transportation Research Board, 1978.
18. Say, M.G., *Alternating Current Machines*, John Wiley and Sons, New York, 1983.
19. Levi, E., *Polyphase Motors: A Direct Approach*, John Wiley and Sons, New York, 1984.
20. Englemann, R.H., *Static and Rotating Electromagnetic Devices*, Marcel Dekker, Inc., New York, 1982.

APPENDIX A

COMPARISON TO OTHER TRANSPRAPHIC GUIDEWAY DESIGNS

